THE REPUBLIC OF TÜRKİYE

MUĞLA SITKI KOÇMAN UNIVERSITY

GRADUATE SCHOOL OF NATURAL AND APPLIED SCIENCES

DEPARTMENT OF METALLURGY AND MATERIALS ENGINEERING

SYNTHESIS AND CHARACTERIZATION OF NANOSTRUCTURED TUNGSTEN OXIDE-SILICON DIOXIDE COMPOSITE COATINGS VIA SOL-GEL DIP COATING TECHNIQUE

MUHAMET NECAR

MASTER THESIS

JANUARY 2025

MUĞLA

MUGLA SITKI KOÇMAN ÜNİVERSİTESİ

Graduate School Of Natural And Applied Science

THESIS ACCEPTANCE APPROVAL

The thesis, submitted by MUHAMET NECAR entitled SYNTHESIS AND CHARACTERIZATION OF NANOSTRUCTURED TUNGSTEN OXİDE-SILICON DIOXIDE COMPOSITE COATINGS VIA SOL GEL DIP COATING TECHNIQUE" has been accepted on Day/Month/Year in fulfilment of Master's Degree in the Department of METALLURGICAL AND MATERIAL ENGINEERING by the thesis committee listed below.

THESIS DEFENCE COMMITTEE

Assist. Prof. Dr. Tolga Tavşanoğlu (**Advisor**) Signature:

Department of Metallurgical and Materials Engineering,
Muğla Sıtkı Koçman University, Muğla _____

Assoc. Prof. Dr. Aslı Çakır (**Jury Chair**)

Signature:

Department of Metallurgical and Materials Engineering,
Muğla Sıtkı Koçman University, Muğla _____

Assoc. Prof. Dr. M. Şeref Sönmez (**Member**)

Signature:

Department of Metallurgical and Materials Engineering, _____
Istanbul Technical University, Istanbul

DEPARTMENT APPROVAL

Prof. Dr. Ali Arslan Kaya (Head of Department) Signature:

Department Of Metallurgy and Materials Engineering,
Muğla Sıtkı Koçman University, Muğla _____

Assist. Prof. Dr. Tolga Tavşanoğlu (**Advisor**) Signature:

Department Of Metallurgy and Materials Engineering,
Muğla Sıtkı Koçman University, Muğla _____

Date of Defence: 28/01/2025

I affirm that all results, documents, information, and files presented in this thesis were obtained by me during my research and adhere to scientific and academic ethical standards. Moreover, I attest to the fact that any other people's original data and findings not arrived at during the research study of this thesis have been cited according to academic and scientific ethic rules.

MUHAMET NECAR

Signature

ÖZET

NANOYAPILI TUNGSTEN OKSİT-SİLİSYUM DİOKSİT KAPLAMALARIN SOL-JEL DALDIRMALI KAPLAMA YÖNTEMİYLE ÜRETİMİ VE KARAKTERİZASYONU

MUHAMET NECAR

Yüksek Lisans Tezi

Fen Bilimleri Enstitüsü

Metalurji ve Malzeme Mühendisliği Anabilim Dalı

Danışman: Assist. Prof. Dr. Tolga Tavşanoğlu

OCAK, 55 sayfa

Tungsten oksit, geniş bant aralığı, kübik, triklinik, monoklinik, ortorombik, tetragonal ve altıgen kristal yapıları, kimyasal stabilitesi, optik ve elektriksel özelliklerinin avantajlı bir karışımına sahip çok yönlü bir malzeme olarak özellikle son on yılda büyük ilgi görmüştür. Özel bir uygulama için özelliklerini optimize etmek amacıyla nanoyapılandırma, katkılama, diğer oksitlerle birleştirme ve kristal faz yerine amorf faz kullanma yaygın yöntemlerdir. Bu çalışmada, nanokompozit tungsten oksit-silisyum dioksit ince filmleri, tek aşamalı sol-jel hazırlama ve daldırma kaplama ile sentezlendi. Çözeltiyi hazırlamak için tungsten kromat, baz kataliz koşulunda amonyum hidroksit ilavesiyle tetra etil orto silikat ve alkol içerisinde çözüldü. Filmlerin mikroyapısal özellikleri SEM gözlemleri ile karakterize edilmiştir. Filmlerin optik özelliklerini ölçmek için spektrofotometre kullanılmıştır. Nanokompozit filmlerin fotokatalitik aktivitesi, temas açıları ve yapay gün ışığı ışınımı altında metilen mavisinin bozunmasının gözlemlenmesiyle değerlendirildi.

Anahtar Kelimeler: Tungsten oksit, Nanokompozit kaplamalar, Sol-jel daldırmalı kaplama, Mikroyapısal özellikler, Optik özellikler, Fotokatalitik özellikler

ABSTRACT

SYNTHESIS AND CHARACTERIZATION OF NANOSTRUCTURED TUNGSTEN OXIDE-SILICON DIOXIDE COMPOSITE COATINGS VIA SOL-GEL DIP COATING TECHNIQUE

MUHAMET NECAR

Master of Science (M.Sc.)

Graduate School of Natural and Applied Sciences

Department of Metallurgy And Materials Engineering

Supervisor: Assist. Prof. Dr. Tolga Tavşanoğlu

JANUARY, 55 pages

Tungsten oxide has attracted lots of attention especially during the last decade as being a versatile material with an advantageous mixture of wide band gap, crystal structures: cubic, triclinic, monoclinic, orthorhombic, tetragonal, and hexagonal; optical and electrical characteristics; chemical stability. To optimize its properties for a specific application, nano-structuring, doping, combining with other oxides, and using an amorphous phase instead of a crystalline phase are common methods. In this study, nanocomposite tungsten oxide-silicon dioxide thin films were synthesized with one step sol-gel preparation and dip coating. To prepare the solution, tungsten chromate was dissolved in tetra ethyl ortho silicate and alcohol in base catalysis condition by the addition of ammonium hydroxide. The microstructural properties of the films were analyzed using SEM observations. Spectrophotometers were utilized to measure the optical properties of the films. The photocatalytic activity of the nanocomposite films was assessed by monitoring the contact angles and the degradation of methylene blue under artificial daylight irradiation.

Keywords: Tungsten oxide, Nanocomposite coatings, Sol-gel dip coating, Optical properties, Microsttructural properties, Photocatalytic properties.

To My Father Soul

ACKNOWLEDGEMENT

I would like to thank Assist. Prof. Dr. Tolga Tavşanoğlu for his patience during my studies, the facilities and opportunities he provided, and his unwavering support in all circumstances and difficulties. I am grateful to him for being my role model, inspiring me at every step of my academic journey. Just like in this thesis, every success I achieve will bear his influence. I am honored and content to have been one of his students.

I am forever grateful to my family for their affection, blessings, and concern for me to instruct and equip me for my forthcoming days.

TABLE OF CONTENTS

LIST OF TABLES

LIST OF FIGURES

LIST OF ABBREVIATIONS

O	Oxygen
MIC	Metal-Induced Crystallization
G	Gibbs Free Energy
PLD	Pulsed Laser Deposition
TEOS	Tetraethyl Orthosilicate
SEM	Scanning Electron Microscope
IR	Infrared Radiation
WO_3	Tungsten Oxide
2Ɵ	X-Ray Beam Angle
SPC	Solid Phase Crystallization
T°C	Critical Temperature
W	Tungsten
SIO_2	Silicon Dioxide
CVD	Chemical Vapor Deposition
LPC	Liquid Phase Crystallization
K	Kelvin Temperature Transition
WO_2	Tungsten Dioxide
MIT	Metal-Insulator Transition
H	Enthalpy
S	Entropy
O	Oxygen
DC	Direct Crystallization
XRD	X-Ray Diffraction
°C	Temperature
M(OR)n	Metal Alkoxide

1. INTRODUCTION

Tungsten oxide (WO_3) is renowned for its diverse oxidation states, which give rise to various oxides like WO_2 and WO_3, each with distinct structural, optical, and chemical properties. Notably, at elevated temperatures, tungsten oxide undergoes a transition from a semiconductor to a metallic state, significantly changing its electrical and optical properties.This phenomenon involves a structural shift from a low-temperature setup to a high-temperature tetragonal configuration (Thorsten Wagner, 2000). In its monoclinic phase, tungsten oxide exhibits non-metallic properties and infrared transparency at room temperature but becomes metallic and reflective to infrared radiation upon heating (Livage et al., 1988).

Despite extensive research, the mechanisms underlying these phase transitions in tungsten oxide remain not fully understood. However, its ability to undergo reversible metal-insulator transitions makes it valuable in applications such as gas sensors, smart windows, photocatalysis, and electrochromic devices (Claes G. Granqvist, 1995). Multiple synthesis methods, Various methods, including hydrothermal synthesis, sputtering deposition, chemical vapor deposition, pulsed laser deposition, and the sol-gel process, have been developed to produce high-quality materials., phase-specific tungsten oxides. The sol-gel method, in particular, is a low-temperature chemical route that synthesizes ceramic materials through the polycondensation of monomers into a colloidal mixture, eventually forming a network of nanoparticles or a polymerized bulk network (W. A. MacDonald, 1992).

This technique is crucial for creating coatings with exceptional technical properties such as heat insulation, low dielectric constant, and strong visible light transmission. Tungsten oxide coatings are being increasingly utilized in optical, magnetic, and thermal applications, including applications like anti-reflective coatings and thermal insulation. Their dielectric properties make them suitable for various microelectronic structures, enhancing their appeal for optical coatings, microelectronics, optoelectronics, photocatalysis, self-cleaning surfaces, solar energy technologies,

Tungsten oxide coatings are increasingly employed in optical, magnetic, and thermal applications(Arendt & Wilkinson, 2000).

On the contrary, The most researched electrochromic material is tungsten oxide among n-type semiconductors due to its excellent electrochromic properties in the visible and infrared ranges, cost-effectiveness, and high color efficiency. Tungsten oxide films exhibit various chromogenic characteristics, including photochromism and electrochromism, with some irreversible coloration processes (Späth et al., 2007). These films are widely used in electrochromic devices as cathode materials due to their superior reflective properties in the near-infrared spectrum for thermal modulation and transmissive properties in the visible range for transmission modulation. The electrical characteristics of tungsten oxide thin films are crucial for gas sensor applications, where both crystalline and amorphous forms are utilized (Kim et al., 2006). Several fabrication techniques exist for tungsten oxide thin films, including physical vapor deposition, sputtering, thermal evaporation, spray deposition, sol-gel, and electrodeposition .

Silicon dioxide (SiO_2) coatings, renowned for their electrochromic and photochromic attributes, these materials are extensively utilized across multiple industries because they integrate light-responsive photochromic features with electrochromic properties that react to electric fields.These coatings offer benefits like solar control, energy savings, and visual comfort. The sol-gel method, in particular, is favored for producing tungsten oxide and silicon dioxide thin films due to its low cost, lack of special conditions, versatility in starting materials, ability to produce homogeneous thin films, and capability to cover substrates with varying characteristics and sizes .

This technique allows for the modification of solution concentration, gel formation time, annealing temperature and duration, and doping with various metals to produce thin films with diverse thicknesses and physical properties, making it essential for optical and electrical applications (Livage et al., 1988).

In this study, nanocomposite tungsten oxide-silicon dioxide thin films were synthesized with one step sol-gel preparation and dip coating. To prepare the solution, tungsten chromate was dissolved in tetra ethyl ortho silicate and alcohol in base catalysis condition by the addition of ammonium hydroxide. The microstructural properties of the films were analyzed using SEM observations. Spectrophotometers

were utilized to measure the optical properties of the films. The photocatalytic activity of the nanocomposite films was assessed by monitoring the contact angles and the degradation of methylene blue under artificial daylight irradiation.

2. THEORETICAL BACKGROUND

2.1. Tungsten Oxide

Tungsten oxide, characterized by its body-centered cubic structure with a lattice parameter of 3.16 Å, is predominantly present in the +6 oxidation state, as evidenced by its electronic configuration of [Xe]5d46s2. Within the WOx series, encompassing a range of oxides, including WO_2 with a monoclinic structure and polymorphic WO_3, which exists in multiple phases, the compound demonstrates variability with x ranging from 2 to 3. These oxides are renowned for their diverse optical, structural, and chemical characteristics, with phase transitions from semiconductor to metal occurring under the influence of factors like temperature, electric fields, or doping; the tungsten-to-oxygen ratio crucially influences the material's structure and properties. Tungsten trioxide (WO_3) is distinguished by its capacity to shift from a semiconductor to a metal in the vicinity of room temperature, particularly at approximately 68°C, adopting a tetragonal structure in its metallic form and a monoclinic structure in its semiconducting form. The configuration of WO_3 overall resembles that of a perovskite structure devoid of the 'A' atom, as depicted in (Figure2.1.) featuring a network of WO_6 octahedra, the structure's various phases result from discrepancies in the tilting patterns, deformations, and the arrangement of the central tungsten atoms within the octahedra (Linderälv, n.d.).

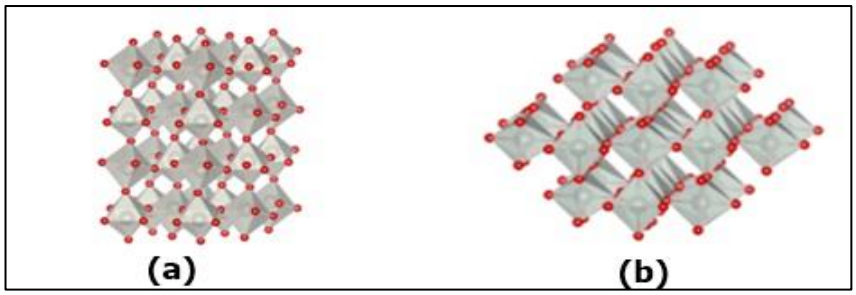

Figure 2.1. (a) Monoclinic WO_3 octahedron configuration. (b) Octahedron WO_2 octahedron configuration

A. Cremonesi et al. (2008) investigated the electrochromic properties of WO_3 thin films that were produced using the sol-gel dip coating method. High annealing temperature (≥300 ˚C) has resulted in a large amount of Na+ ions incorporation in the film and reduction in the electrochromic efficiency.

Nilgun Ozer (1997) employed the sol-gel spin coating method to prepare amorphous WO_3 thin films. The study's findings indicate that the chemistry of the solution significantly influences both the refractive index and the electrochromic coloration of the films. The films show high transmittance and low absorption in the visible region (extinction coefficient, k = 5.6 × 10^-3; and refractive index, n = 1.96).

Esra Ozkan Zaim and Fatma Tepehan (2002) studied By analyzing the structure and optical properties of porous WO_3 thin films prepared using the sol-gel spin coating technique through X-ray diffraction, it was observed that the tungsten oxide film begins to crystallize at an annealing temperature of 350 ˚C. The peaks appeared at 23.14˚, 23.64˚ and 24.36˚ corresponding to (002), (020) and (200) diffractions in the triclinic structure. The refractive index was found n = 2.00 at wavelength, 550 nm and n = 1.97 at 633 nm. The value was lower in the porous structure. The extinction coefficient was found k = 8.8 × 10-5 at 550 nm and k = 4.11 × 10-3 at 633 nm.

Esra Ozkan Zaim and F.Z. Tepehan (2001) studied the optical properties of WO_3 thin films (prepared using the spin coating technique) within the wavelength range of 200–1100 nm. They concluded that the optical transmittance decreases with increasing film thickness. The transmittance values increase from 0% to 60% in the wavelength region 300–400 nm with a sharp peak at 350 nm, and from 60% to 80% in the range 400–1100 nm. It was also noted that the surface roughness increases with the number of coatings applied. Additionally, the refractive index and extinction coefficient change based on the chemical composition and thickness of the films. For 6-layer coated film (thickness, 580 nm) at wavelength, 550 nm The refractive index and extinction coefficient were determined to be n = 1.77 and k = 1.395 × 10-3, respectively, While for 7-layer coated film (thickness, 675 nm) n = 1.89 and k = 0.984 × 10-3.

Solution chemistry is easily tunable to affect the optical and morphological properties of the WO_3 thin films with an optical band gap of 3.10 ± 0.12 eV. D. Saygın et al. (2008) investigated the WO_3 thin films which were fabricated by sol-gel method and spin coating technique at different annealing temperatures (250 and 400 ˚C). The WO_3

films were amorphous at annealing temperatures of 250 and 400 ˚C. The optical properties showed a refractive index of n = 1.96 ± 0.02 (250 ˚C) and n = 1.94 ± 0.08 (400 ˚C) at a wavelength of 550 nm in the range of 300 to 1000 nm. The optical transmittance was increased from 30% to 70% in the 300 to 400 nm range and from 70% to 80% in the 400 to 1000 nm range. The optical reflectance increased from 10% to 20% in the 300 to 400 nm range, while it decreased from 20% to 15% in the 400 to 1000 nm range. The optical transmittance was measured as 73% at 550 nm. Lay Gaik Teoh et al. (2005) studied the structure and optical characteristics of porous tungsten oxide thin films coated by sol-gel method. They reported that the films showed monoclinic structure from room temperature up to 330 ˚C. The optical band gap energy of the porous tungsten oxide thin films was 3.5 eV, with increased absorption observed for wavelengths shorter than 360 nm. It was also demonstrated that the films showed photochromic behavior upon UV light illumination. P.K. Biswas et al. (2003) studied the optical characteristics of WO3 thin films (500 nm thickness) coated by sol-gel dipping technique. The optical transmittance was measured between 20 and 30% in the 400 to 800 nm range in the coloration state and 60 to 70% in the whitening state. As the coating thickness decreases, E. Z. Özkan (this study) observed that the interference effect decreases. Kai Huang et al. (2007) investigated the optical, structural and chemical characteristics of WO3 thin films affected by coloration and whitening cycles especially the cyclic efficiency and the degradation during long term cyclic measurement. They reported that the films showed a stable structure after a thousand cycles of coloring and whitening. After 2000 cycles, different degradations and cracks were seen in the crystal structures.

Long-term cyclic measurement was accompanied by the destruction of the electrochromic structure because of the degradation of the surface and crystal structure.

R. Solarska et al. (2006) "WO_3 thin films coated via the sol-gel method. Influence of the starting materials and annealing temperature" J. Non-Cryst. Solids 352 1491–1495 studied the influence of starting materials and annealing temperature on the structure and photoelectrochemical characteristics of WO_3 thin films. Tungstic acid ($H2WO_4$) was used as the starting material and organic compounds were added to the sols. For

better photoelectrochemical properties, the crystal structure of the film must be monoclinic.

C.O. Avellanado et al. (2003) "Optical transmittance of tungsten oxide films coated by the sol-gel immersional technique and annealed in the temperature range 100–150 ˚C under light and an electric field" Thin Solid Films 442 150–155 studied the optical transmittance of WO_3 films prepared by the sol-gel method and annealed at 100–150 ˚C. The films were coated onto glass substrates by the immersional technique from tungstic acid sols with different concentrations. Crystallization of the amorphous films started at about 450 ˚C. The diffractogram showed peaks at 23˚ which can be indexed to (200), (020) and (002) planes. The photochromic effect of the films was studied in the wavelength range $300 < \lambda < 2100$ nm. The coloring and whitening processes were carried out at 633 nm. For WO3 thin films, the variation of the optical transmittance (ΔT) between the coloring and whitening process was also studied. A 410 nm thick film at 120 ˚C showed a ΔT value for Ti-doped WO3 thin films, while a 415 nm thick film at 150 ˚C showed a ΔT value of 54%. A 520 nm thick film at 150 ˚C exhibited a ΔT value of 43.39%, while a 550 nm thick film at 120 ˚C showed a ΔT value of 64.49%. All the amorphous films showed photochromic effect.

A. Patra et al. (2004) concluded that electrochromic tungsten oxide thin films, coated by sol-gel dipping method, showed maximum photochromic effect when annealed at 200 ˚C for one hour. Structural and optical properties were investigated at various annealing temperatures, in the range of 60 to 400 ˚C. At low temperature, the film was amorphous and at the optimum annealing At different temperatures, the films displayed an orthorhombic crystal phase with a W-O-W bond structure. X-ray diffraction studies revealed that the sample annealed at 60 ˚C did not achieve complete crystallization, as indicated by its very low peak intensity. In contrast, the sample annealed at 400 ˚C demonstrated clear crystallization and exhibited the orthorhombic crystal phase. Agnihotry (2006) investigated the influence of coloration–whitening cycle on the optical properties of tungsten oxide thin films prepared using the sol-gel dipping process. They observed that the films became whiter during oxidation phase and all the films showed systematic decrease in optical transmittance spectrum in the $300\text{nm} > \lambda > 800\text{nm}$ range. The reduction reaction also induced the variation in optical transmittance. After five coloration cycles, the permeability varied by 1.2% and after

whitening cycle it varied by about 17%. The films showed perfect and irreversible properties during the first five cycles. The coloration efficiency decreases during the reduction process.

2.2. Tungsten Oxide Systems

Tungsten, symbolized by W is a transition metal that creates oxides collectively known as tungsten oxides (WO_x) where x typically ranges between 2 and 3. These oxides have forms with common oxidation states being W^4+, in WO_2 and W^6+ in WO_3. The highest oxygen state in the tungsten oxygen system is represented by WO_3. Between WO_2 and WO_3 there are intermediate nonstoichiometric phases known as Magneli phases, like $W_{18}O_{49}$ and $W_{24}O_{68}$ each distinguished by its unique crystal structures and properties (Louzguine & Inoue, 1999).

Understanding the phase diagram shown in (Fig 2.2.) of tungsten oxides is essential to determine the phases under conditions. This knowledge offers insights into the characteristics of these materials guiding their synthesis and application in various tungsten oxide-based products.Researchers extensively explore tungsten oxides for their capabilities which're beneficial for applications like smart windows and displays. The capacity to change color reversibly when subjected to a field is a trait of these materials. Films of tungsten oxide can be deposited using various methods such as chemical vapor deposition (CVD), sputtering, pulsed laser deposition, epitaxial growth, and the sol-gel technique.These techniques enable the production of films, with porosity, thickness and composition control to enhance the electrochromic performance of the material (Sudo, 1992).

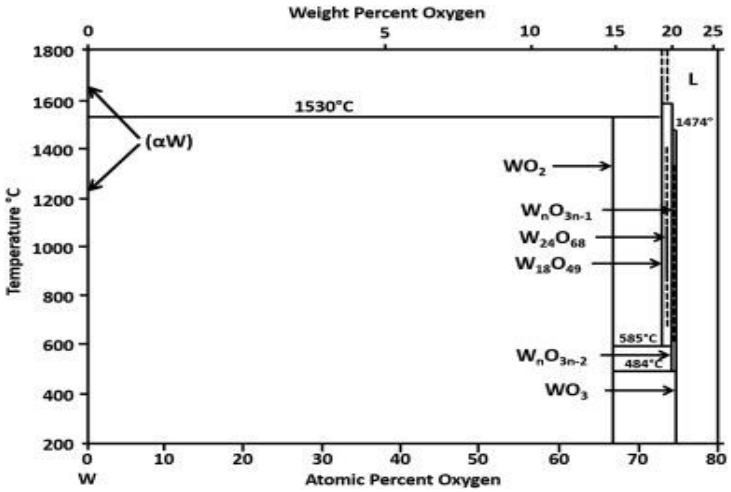

Figure 2.2. Phase diagram of Tungsten Oxide

2.3. Properties of Tungsten Oxides

The properties of tungsten oxide are summarized in Table 2.1.

Table 2.1. Tungsten oxide properties

Property	Tungsten Oxide (WO_3)
Crystal Structure	Monoclinic, orthorhombic, cubic, or hexagonal
Band Gap	2.6 to 3.2 eV (semiconductor)
Optical Properties	Electrochromic, visible light photocatalytic
Photocatalysis	Effective under visible light
Density	~7.16 g/cm³
Hardness	Relatively hard, moderate wear resistance
Thermal Stability	Stable up to ~1,470°C
Corrosion Resistance	Resistant to oxidation, moderate chemical stability
Electrochromism	Strong electrochromic properties
Thermochromism	Color change with temperature
Electrical Properties	n-type semiconductor
Mechanical Properties	Moderate hardness, can be brittle
Chemical Activity	Can be catalytically active

2.3.1. Electrochromism

Cilt In the realm of materials, there exists a fascinating phenomenon known as electrochromism, where materials display reversible color changes due to electrochemical reactions. This phenomenon is part of the broader category of material chromism,alongside thermochromism (color changes due to temperature) and photochromism (color changes due to light exposure). Electrochromism, specifically, refers to color transformations induced by an electric potential. Remarkably, even a minimal electric potential, often requiring only a few volts, or sometimes even less, can trigger these color alterations in electrochromic materials(Zhang et al., 2019).

2.3.1.1. Electrochromism applications

The realm of electrochromic boasts a myriad of practical applications spanning from information displays to optical modulators and intelligent window glazing systems. One notable application lies in the realm of smart windows, where electrochromic technology is leveraged to regulate the ingress of both heat and light. In this configuration, a thin layer of electrochromic material is typically applied onto window glass, facilitating dynamic control over transparency. Moreover, in automotive settings, transmittance modulation via electrochromic mechanisms has been harnessed to automatically adjust the tint of rearview mirrors in response to varying illumination conditions. The depicted pattern comprises five distinct layers, which are either sandwiched between two surfaces or arranged in a stacked configuration. Commonly, these layers are supported by flexible polyester film or glass substrate. Central to this five-layer assembly lies the electrolyte, a pure ion-conducting material. This electrolyte, situated centrally within the structure, can take on either organic form, typically an adhesive polymer or an inorganic compound, often based on oxide sheets (Kosinski, 2005). Hydrogen ions (H+) or lithium ions (Li+) are frequently favored as ion carriers due to their diminutive size, which enables mobility within the structure as shown in (Figure 2.3.).

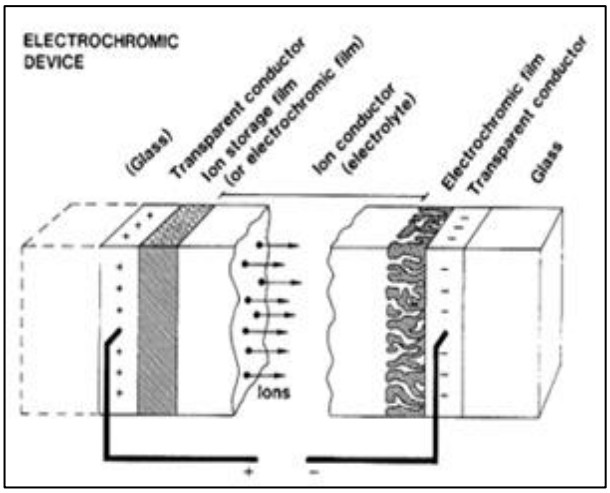

Figure 2.3. The fundamental layout of an electrochromic device

2.3.1.2. Advantages

- Dynamic Control of Light and Heat: Electrochromic coatings have the distinctive capability to change their color and transparency when an electrical current is applied. This dynamic responsiveness enables precise regulation of both light and heat transmission. Consequently, electrochromic coatings find optimal utility in the realm of smart windows, adept at darkening to mitigate sunlight and heat or lightening to facilitate natural illumination and warmth(Jabur & Al-Fatlawi, n.d.).
- Enhanced Energy Efficiency: By mitigating solar heat gain during warmer seasons and reducing reliance on artificial lighting, electrochromic coatings play a crucial role in enhancing the energy efficiency of buildings. This translates to tangible benefits such as diminished energy expenditures and mitigated greenhouse gas emissions.
- Privacy and Security Enhancement: Electrochromic windows offer the versatility of transitioning into an opaque state, catering to privacy and security requirements. This feature is especially beneficial in environments like conference rooms, office spaces, and residential environments where privacy is paramount.
- Durability and Low Maintenance: Notably robust, electrochromic coatings exhibit high durability and necessitate minimal upkeep. Unlike conventional window

tinting films, they are impervious to UV-induced fading or degradation, thereby ensuring prolonged functionality with minimal maintenance demands.

2.3.1.3. Disadvantages

- Cost: Presently, Electrochromic coatings generally involve higher expenses compared to conventional window tinting films or blinds. Nevertheless, as technology matures, there is a notable trend towards cost reduction. Moreover, the long-term energy savings facilitated by these coatings can potentially offset the initial investment.
- Complexity: Implementing electrochromic systems necessitates the incorporation of electrical wiring and controls, thereby augmenting the intricacy associated with both installation and maintenance processes.
- Switching Speed: The rate at which electrochromic coatings change colors can differ based on the particular material used and the voltage applied. In certain cases, the switching process may require several seconds to complete.
- Limited Color Range: While certain electrochromic coatings offer versatility in transitioning across a spectrum of colors, the available range is presently constrained when juxtaposed with traditional window tinting films. (Zhang et al., 2019), (Granqvist et al., 2003).

2.3.2. Photochromism

Reversible Photosensitivity in Materials. Certain materials exhibit a fascinating phenomenon known as photochromism. This property manifests as a reversible change in color upon exposure to ultraviolet (UV) radiation. Two primary categories of materials showcase this intriguing behavior.

In the domain of ophthalmic applications, specifically designed glasses incorporate metal halides as the active component within their melt. These inorganic photochromes, however, are limited in their color palette because of the lack of appropriate coating materials for organic polymer substrates.

Alternatively, organic polymers can be imbued with photochromic properties through the inclusion of organic dyes such as spirooxazines, spiropyrans, chromenes, and dihydroindolizines. Recent advancements in thermal transfer techniques have opened the door to the development of photochromic polymeric lenses utilizing these organic dyes. This approach offers greater versatility in color expression compared to traditional inorganic materials(Ahmadi et al., 2020).

2.3.2.4. Advantages

- Eye Protection: In eyewear, photochromic coatings are beneficial for reducing glare and eye strain by adjusting the level of tint based on sunlight intensity. This dynamic tinting helps shield the eyes from harmful UV rays, offering enhanced protection.
- UV Protection: Photochromic coatings typically provide robust UV protection, which is essential for preventing harm to the eyes from ultraviolet radiation.
- Adaptability to Light Conditions: These coatings offer automatic adjustment to changing light conditions. They darken in response to UV light and return to their original clear state when UV light is no longer present, ensuring optimal visual comfort(Iwai et al., 2014).

2.3.2.5. Disadvantages

- Reaction Time: The response time of photochromic coatings can vary, with some coatings taking longer to transition between clear and tinted states. This delay can be a drawback in scenarios where rapid adaptation to changing light conditions is necessary.
- Temperature Dependency: The performance of some materials can be influenced by temperature variations. In colder temperatures, the activation or transition speed may slow down, impacting their effectiveness.
- Cost: Products incorporating photochromic Coatings are often more expensive than non-photochromic alternatives, which may be a factor for consumers considering cost-effectiveness (Tong Cheng et al., 2007), (Cheng et al., 2008).

2.3.3. Structure

The study of stoichiometric tungsten trioxide reveals that when heating or cooling, phase transitions and structural polymorphism take place at distinct temperatures. The monoclinic I (γ-WO_3) phase is the stable form most commonly observed at room temperature, existing within the temperature range of 17–330°C. Below room temperature, two more crystallographic phases exist: monoclinic II (ϵ-WO_3) for $T < -43$ °C and triclinic (δ-WO_3) for -43 °C $< T <$ 17 °C. γ-WO_3 becomes orthorhombic β-WO_3 (stable to 740°C) when heated above 330°C, while tetragonal α-WO_3 is discovered at $T >$ 740°C. Nevertheless, these two phases are only stable at exceptionally high temperatures, and they return to γ- WO_3 when cooled. Additionally, a metastable hexagonal phase (h- WO_3) can be synthesized chemically using various techniques. This hexagonal phase transforms into γ- WO_3 when heated above 400 °C and then cooled. When impurities such as hydrogen, sodium, or lithium are present, a cubic phase (c-WO_3) is observed in powders and thin films, coexisting with the monoclinic phase. While this cubic phase is deemed ideal at high temperatures, it has not been detected in bulk samples and thus serves as a structural reference for WO_3.The cubic WO_3 (c-WO_3) structure, illustrated in the figure below, resembles the ReO3-type and consists of WO_6 octahedra linked at their edges and corners. The different polymorphs of WO_3 are known as distorted ReO_3 structures, arise from different tilting angles and rotations of these WO_6 octahedra. These octahedral units collectively form a structure resembling perovskite as shown in (Figure 2.4.) for instance, in h-WO_3 Tunnels along the c-axis are formed as a result of the sharing of corner oxygen atoms in configurations of six- and three-membered rings (Mardare & Hassel, 2019a).

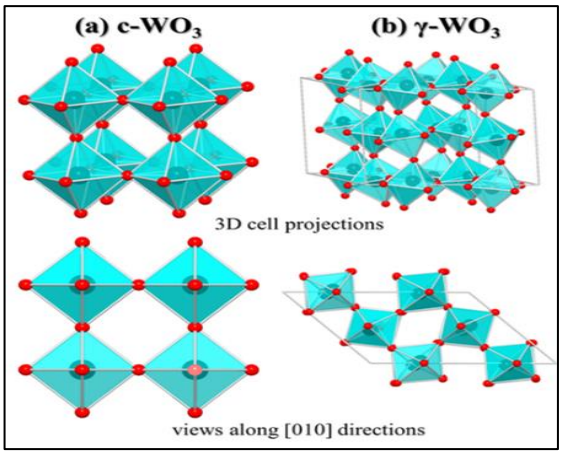

Figure 2.4. Cell projections showing views

Crystal structure remodeling creates stoichiometric oxides, such as the Magneli phase, since there are less oxygen atoms in the crystal structure. (Figure 2.5.) displays the O-W phase diagram varies as a function of temperature, emphasising the different oxygen concentration ranges containing the Magneli phases.

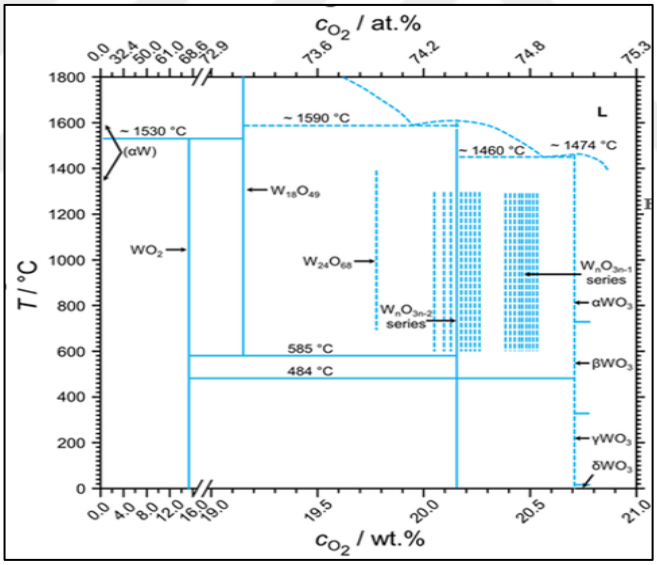

Figure 2.5. Oxygen-Tungsten phase diagram

Whereas shared edges and even surfaces gradually arise for the sub stoichiometric oxides as the oxygen level decreases, the WO_6 octahedra shares only the corners for the stoichiometric WO_3. The defining features of these oxides are edge-sharing WO_6 octahedra, which create channels forming pentagonal columns and hexagonal tunnels. An illustration of this kind of crystallographic structure for $W_{18}O_{49}$ is depicted in (Figure 2.6.).

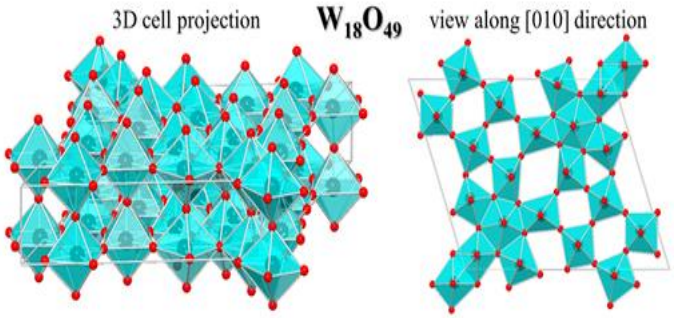

Figure 2.6. An illustration of the $W_{18}O_{49}$ Magneli phase's crystalline structure in three dimensions

The ability of a material to act as a photocatalyst is a key factor in environmental and energy applications. WO_3 is highly active under visible light, which makes it particularly useful in photocatalytic applications such as water splitting, air purification, and the degradation of organic pollutants. The effectiveness of WO_3 in these processes is attributed to its ability to generate reactive oxygen species upon light absorption, which can degrade harmful compounds.

In contrast, SiO_2 is chemically inert and does not exhibit any photocatalytic activity. However, its inert nature is advantageous when SiO_2 is used as a support material or matrix in composite structures. In the synthesis of WO_3-SiO_2 composite coatings, SiO_2 can provide structural stability and mechanical reinforcement, while WO_3 serves as the active photocatalytic component. The incorporation of SiO_2 ensures that the composite maintains its structural integrity, even under prolonged exposure to light or in reactive environments.

2.3.4. Chemical and physical properties

To create crystalline tungsten trioxide, (Reaction 1). Ammonium paratungstate tetrahydrate or tungstic acid (Reaction 2) are calcined in air at temperatures above 400 °C. The resulting chemical changes occur due to the following decomposition processes:

$$(NH_4)_{10}(H_2W_{12}O_{42}).4H_2O \xrightarrow{T\rangle 400\ ℃} 12WO_3 + 10NH_3 + 10H_2O\ (Reaction1).$$

$$(NH_4)_{10}(H_2W_{12}O_{42}).4H_2O \xrightarrow{T\rangle 400\ ^\circ C} 12WO_3 + 10NH_3 + 10H_2O\ (Reaction 1).$$

The powder that is formed when stoichiometric WO_3 is produced is yellow in colour and turns green when there is a deficit of oxygen. The magnéli phases arise at high temperatures when WO_3 is reduced in moist H_2. Based on the stoichiometry, these phases exhibit different colors: bluish-violet for $WO_{2.9}$, reddish-violet for $WO_{2.72}$, and brown for WO_2.Tungsten trioxide has a wide range of stable pH values, from neutral to acidic, according to the Pourbaix diagram furthermore, it is hardly soluble in acidic conditions and has significant (photo) electrochemical stability in them, has a rather high melting point of 1473 °C; below this temperature, it starts to sublimate, especially when water vapour is present (Mardare & Hassel, 2019b).

A large bandgap n-type semiconductor with d0-transition metal oxide properties is tungsten trioxide. The electron concentration is mainly determined by inherent defects, such as oxygen vacancies (VO_{2+}), which have a concentration in the range of 10^{13}–10^{17} cm^{-3}. The electronic bandgap (Eg) is the energy gap separating the valence band and the conduction band. The valence band is formed by fully occupied O 2p orbitals, while the conduction band consists of unoccupied W 5d orbitals, as illustrated in (Figure 2.7.) the electronic bandgap value of bulk γ-WO_3 is around 2.6–2.8 eV. This number is influenced by the extent of distortion from the cubic structure to amorphous WO_3 has a significantly broader bandgap of ≈3.2 eV. The bandgap values increase even more as WO_3's size is lowered into the nanoscale region because of quantum confinement. WO_3 the ability to absorb around 12% of solar radiation42, ranging from ultraviolet to 400 nm in wavelength. WO_3 is not conducive to one-step hydrogen generation due to its reduction potential, as assessed against the standard hydrogen electrode (SHE). The edge of the conduction band (CB) is below the threshold for photocatalytic hydrogen evolution. WO_3 can promote the production of oxygen, nevertheless, because The valence band (VB) potential is situated at around 3.2 eV in relation to SHE. Because of its property, it is a material that is much sought after The valence band (VB) potential is crucial when considering its application as a photoanode in photoelectrochemical water splitting. The VB position promotes the formation of hydroxyl radicals, which allows for the oxidation of organic pollutantsThe same mechanism also underlies its antibacterial action, as hydroxyl

radicals are associated with cell membrane damage, leading to the inhibition of bacterial growth (Mardare & Hassel, 2019a),(Granqvist, 1999).

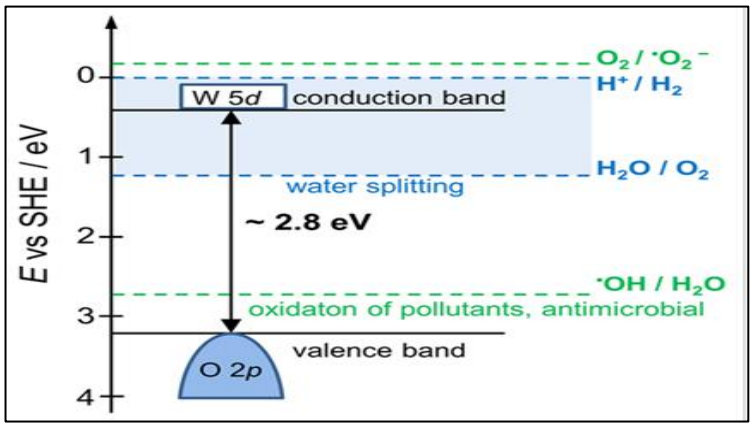

Figure 2.7. Boundaries of the valence and conduction bands of WO_3

Migas et al. conducted Ab initio calculations to determine the electric properties of Magneli phases. The metallic properties shown by these materials are attributed to the placement of Fermi levels that intersect certain energy bands that exist within each substoichiometric oxide discussed earlier.

WO_3's optical properties are closely linked to its bandgap. Since there is no absorption in the visible spectrum or for light wavelengths longer than 400 nm, WO_3 looks transparent to brilliant yellow. Interbrand transitions occur at shorter wavelengths where photon energy values exceed the bandgap energy. According to Gullapalli, the ultraviolet to blue part of the spectrum is where the absorption threshold is located. In oxygen-deficient phases (also known as Magnelli phases), vacancies in oxygen generate additional energy bands beneath the conduction band, these vacancies exhibit an absorption band in the near-infrared region, imparting a green to bluish coloration (Niklasson et al., 2004).

2.3.5. Transition from metal to insulator in tungsten oxide

Tungsten oxide (WO_x) captivates researchers with its ability to undergo a dramatic metamorphosis referred to as the Metal-to-Insulator Transition (MIT). This phenomenon signifies a drastic shift in its electrical properties, where the material transforms from a conductor of electricity (metallic) to an insulator (resistant to current

flow) or vice versa. This essay delves into the captivating intricacies of this transition from a condensed matter physics perspective.

Within the realm of condensed matter physics, metals and insulators represent distinct classes of materials. This distinction arises not only from their contrasting electrical behaviors but also from their underlying crystal structures. Metals generally possess high coordination numbers, often 8 or 12, signifying the number of nearest neighbor atoms they interact with. Conversely, insulators exhibit lower coordination numbers, often explained by "octet rule" bonding arrangements, where each atom forms bonds with enough neighboring atoms to achieve a stable configuration with eight electrons in its outermost shell. Classic examples include crystalline silicon (Si) and germanium (Ge) with their diamond structures, where each atom boasts four nearest neighbors, resulting in an octet of valence electrons. Lead (Pb), on the other hand, exemplifies a material that perpetually remains metallic (Clarke, 2008).

However, the element tin (Sn) throws a captivating curveball. Gray tin, possessing a diamond structure, behaves as a brittle semiconductor with a narrow bandgap, whereas white tin, adopting a body-centered tetragonal structure, manifests as a malleable metal. These two forms – gray and white tin – exist in a delicate energetic balance. The transformation from metallic white tin to semiconducting gray tin occurs at low temperatures, a phenomenon historically known as "tin pest" or "tin blight." This peculiar transition caused organ pipes constructed from tin to crumble and disintegrate in 18th-century Europe (Bauer et al., 2003).

The essence of this phenomenon revolves around the concept of orbital overlap. Theoretical predictions suggest that all insulators, under sufficiently high pressure or density, should transform into metals. Experimentally achieving such pressures to induce this transition, however, remains a significant challenge. Silicon and germanium, for instance, stubbornly persist as semiconductors (insulators) under attainable conditions. However, because of the complex interplay of electrical interactions within its atomic structure, tin defies this trend.

To delve deeper into the MIT phenomenon, we can employ the Hubbard model. Imagine a simplistic chain of N atoms, each harboring a solitary valence electron (like hydrogen, sodium, or cesium). According to the basic band theory, such a chain should

exhibit metallic behavior because the N atoms combine to form N orbitals, and the N valence electrons perfectly half-fill these orbitals. However, most materials reside comfortably either in the metallic or insulating regime., far from this critical transition point. The periodic trend observed among transition metal monoxides (MO, where M represents elements from titanium to nickel) exemplifies this concept. Despite sharing the same NaCl crystal structure, these materials exhibit diverse electronic behaviors. (Figure 2.8.) illustrates the electron hopping mechanism in a one-dimensional chain of atoms.

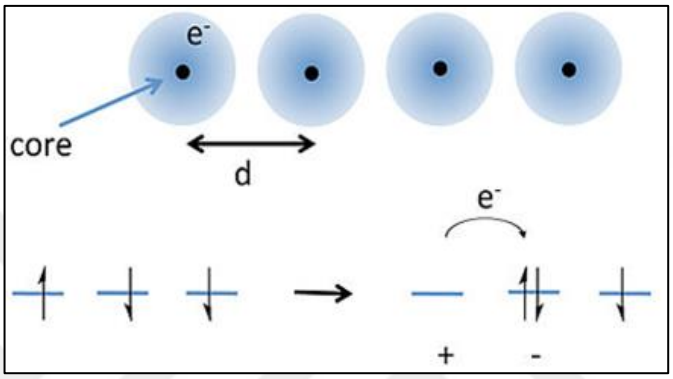

Figure 2.8. Electron hopping in a 1-D chain of atoms

2.3.6. Li intercalation

Tungsten oxide ($WO_3 \cdot nH_2O$) is a notable layered oxide material with diverse applications, particularly in electrochromic devices and energy storage systems. A fascinating feature of this material is the Metal-to-Insulator Transition (MIT), which causes a notable change in the electrical characteristics of a material from metallic to insulating states or the opposite. This discussion explores the specific dynamics of lithium intercalation within tungsten oxide.

Layered Structure: Tungsten oxide features a layered architecture consisting of corner-sharing WO_6 octahedra. The synthesis conditions have an impact on its crystallization into many phases, including orthorhombic, cubic, tetragonal, triclinic, and monoclinic (Xu et al., 2018).

Role of Interlayer Water: The interlayer water in tungsten oxide facilitates high-rate electrochemical proton intercalation. This water presence helps stabilize the structure by reducing electrochemical deformation.

Lithium Intercalation: Introducing lithium ions (Li^+) into the interlayer spaces of tungsten oxide leads to several interesting phenomena:

Hexagonal Structures: Hexagonal tungstates, including oxides or tungsten compounds, demonstrate superior cycling behavior and higher specific capacities during lithium-ion intercalation compared to their monoclinic counterparts.

Pre-Allocated Lithium: The presence of pre-allocated lithium (as Li_2O) in hexagonal tungstate's significantly influences their lithium intercalation capacity(Hu et al., 2017).

2.4. Synthesis Techniques Of Tungsten Oxide

- Doping: It is crucial to create materials that can capture and use a substantial percentage of the sun spectrum in order to meet the growing need for energy. Due to its availability and appealing qualities, tungsten trioxide has attracted a lot of attention in this regard. Extensive research on the bandgap engineering of tungsten trioxide has revealed that its electronic properties can be tuned through appropriate doping. Specifically, bandgap reduction or edge shifting can be achieved by introducing dopants, which modify the electrical characteristics. Studies have shown that cation doping (e.g., Ag, Cr, Hf, Mo, Pt, Ti, Zr) can either reduce the bandgap by elevating the valence band edge or create additional energy states within the bandgap through impurity introduction (Besozzi et al., 2019a).
- Sol-gel: One of the most well-known wet-chemistry coating processes, the sol-gel technique, has drawn a lot of interest in the last 20 years because of its affordability and broad coverage capabilities. These attributes make the sol-gel method particularly attractive for commercial applications. Utilising molecular precursors to produce an oxide network by polymerization is the basis of the technique. These molecular precursors can be inorganic precursors such as metal salts in aqueous solutions, like tungstic acid powder in hydrogen peroxide, or metal alkoxides dissolved in appropriate organic solvents, like $WOCl_4$ in isopropyl alcohol or tungsten oxo-tetra-n-butoxide ($WO(OnBu)_4$) in ethanol. Once the sols are formed, they can be applied to substrates through spraying, spin-coating, or dip-coating

techniques. Stoichiometric and crystalline WO_3 films are obtained by the subsequent hydrolysis, calcination and drying steps. For photoelectrochemical studies, Yang examined the mesoporous films formation of an aqueous precursor based on peroxopolytungstic acid with pH as a parameter. The surface properties, electrochromic and photoactivity of WO_3 can be controlled by the post-deposition heat treatment and the addition of some organic additives in the aqueous solutions, such glycerol, mannitol, polyethylene glycol, or ethylene glycol (Besozzi et al., 2019a).

- Electrochemical Deposition: Electrochemical deposition is a particularly appealing coating process because of its multiple advantages, including cost-effectiveness, the capacity to coat huge areas, and precise thickness control. The typical setup consists of two or three electrodes: a cathode, which serves as the conductive substrate where the film is deposited, an anode (commonly platinum), and optionally, a reference electrode in a three-electrode system. The electrochemical cell is filled with an electrolyte solution containing the metal species intended for deposition. This setup operates under direct current (DC), which facilitates the movement of metal ions from the solution to the cathode, where they are reduced and deposited as a film. The microstructure of the deposited film can be meticulously controlled through adjustments in process parameters and electrolyte composition. Following Yamanaka's foundational research in 1987, significant advancements have been made in the electrodeposition of WO_3 films. In 1999, Meulenkamp conducted a comprehensive study on the electrodeposition mechanism of WO_3 from peroxytungstate solutions. Kwong investigated the impact of peroxotungstic acid concentration and deposition time on the structure and photoelectrochemical properties of WO_3 films. Furthermore, the use of seed layer-coated FTO substrates for electrodepositing nanoflake array films has demonstrated enhanced electrochromic properties and increased sensitivity to H2S (Besozzi et al., 2019b).
- Thermal Evaporation: Thermal evaporation is a widely utilized physical vapor deposition (PVD) technique employed for applying coatings. In thermal evaporation, the source material is typically a metal or metal oxide heated to a sufficient degree to evaporate or sublime. The atoms ejected from the source

proceed radially outward and are incident on a substrate. Tungsten oxide films can be produced using metallic tungsten (W) or tungsten trioxide (WO_3) in the form of powder or pellets as the source material.A metallic coating is first deposited when metallic tungsten is the evaporation source. Annealing in a high oxygen content atmosphere is necessary to produce tungsten oxide upon post-deposition treatment.

As a result, the final coating can exhibit various stoichiometries (x = 2-3), depending on the deposition parameters. Furthermore, the low energy of the species involved in thermal evaporation generally results in oxide films that are amorphous. To obtain crystalline and stoichiometric WO_3, annealing at temperatures up to 400°C is required.

Rough-surfaced WO_3 films produced by evaporation have shown effectiveness in gas-sensing applications. Thermally evaporated WO_3 has also been utilized to fabricate energy storage and electrochromic smart glass windows with exceptional properties(Parreira et al., 2006), (Mardare & Hassel, 2019).

- Sputtering: Another PVD method for thick- and thin-film creation is sputtering. Due to high coating capacity and method versatility, its wide range industrial application is not surprising. The process occurs in a vacuum chamber at 10^{-1} – 10 Pa pressure, with added sputtering gas (He, Ar, Xe, etc.). High-energy ions of sputtering gas (e.g. Ar^+) "knock out" target material atoms, which then deposit on the substrate. Like in thermal evaporation, the source can be either metallic tungsten (W) or tungsten trioxide (WO_3), and can be used both in DC and RF modes. Reactive sputtering can also be performed by introducing varying quantities of O_2 into the sputtering ga. Thus, direct fabrication of tungsten oxide coatings from both metallic and oxide targets with controllable stoichiometry is possible. Heat treatment may be performed both during and after deposition, Reactive sputtering can also be performed by introducing varying quantities of O_2 into the sputtering gas to achieve fully crystalline and/or stoichiometric films.Sputtering parameters like pressure, power density, substrate temperature and oxygen concentration can be easily adjusted for the desired coating stoichiometry, quality and crystallinity (Parreira et al., 2006).

We have chosen the sol-gel coating technique over other deposition methods, including electrochemical deposition, thermal evaporation, and sputtering, for

synthesizing and characterizing our nanostructured tungsten oxide-silicon dioxide composite coatings. This decision is based on several factors that make the sol-gel process particularly advantageous:

- Versatility and Scalability

  The sol-gel process is highly versatile and scalable, providing uniform coatings on large and complex surfaces, which is essential for many applications requiring extensive coverage. Moreover, this method is readily scalable for industrial production, making it appropriate for both laboratory research and large-scale manufacturing applications (Stuart, 2016).

- Cost-Efficiency

  A key advantage of choosing the sol-gel method is its cost-effectiveness. The process does not require expensive materials or equipment. Compared to other deposition techniques, the equipment and materials needed for sol-gel synthesis are relatively inexpensive. This economic advantage is significant for large-scale production, making the sol-gel method attractive for both research and industrial purposes.

- Precise Control Over Composition and Structure

  The sol-gel process enables meticulous control over both the composition and structure of the resulting coatings. By carefully selecting molecular precursors and adjusting processing parameters, we can control the properties of the tungsten oxide-silicon dioxide composite coatings. This level of control is crucial for optimizing functional properties, such as electrochromic and photocatalytic behaviors.

- Low-Temperature Processing

  Another significant benefit of the sol-gel method is its ability to produce high-quality coatings at comparatively low temperatures. This is particularly beneficial for applications involving temperature-sensitive substrates. In contrast, methods like thermal evaporation and sputtering often require high temperatures, limiting their applicability and increasing processing costs (Jeon et al., 2022).

- Homogeneity and Purity

  The sol-gel process ensures high homogeneity and purity of the resulting coatings. The molecular-level mixing of precursors in the sol-gel solution leads to uniform

distribution of components, resulting in coatings with consistent properties throughout. This homogeneity is essential for achieving reliable and reproducible performance in practical applications (Mardare & Hassel, 2019c).

- Adjustability in Coating Applications

  The sol-gel process offers a wide variety of coating application methods, including dip-coating, spin-coating, and spray-coating. In this study, we chose dip-coating for its straightforwardness and its capability to produce uniform coatings on substrates of diverse shapes and sizes. Dip-coating also allows easy control over coating thickness by adjusting the withdrawal speed and sol-gel solution concentration.Overall, the sol-gel coating method provides a unique combination of adaptability, cost-effectiveness, precise regulation of composition and structure, low-temperature processing, and superior consistency. These advantages make it an excellent choice for creating and analyzing nanostructured tungsten oxide-silicon dioxide composite coatings. By harnessing the advantages of the sol-gel method, we aim to produce coatings with improved functional properties that are suitable for a broad spectrum of applications.

2.5. Applications

Tungsten oxide (WO_3) is widely employed across various technological applications because of its exceptional properties. It functions effectively as an antimicrobial agent, in photo (electro) catalysis, sensors, and electrochemistry. The material's photocatalytic qualities make it suitable as a photoanode for water splitting, and its electrochromic and photochromic characteristics make it an excellent candidate for smart windows applications. Furthermore, tungsten oxide functions as a photothermal nanomaterial in cancer treatment, water evaporation, and photocatalysis. It is also essential in applications such as near-infrared (NIR) shielding, gas sensing, and lithium-ion batteries. Its capacity to absorb near-infrared light and convert it into heat presents significant potential for advancements in energy-efficient technologies and healthcare solutions.

Furthermore, significant advancements and market deployment in these areas highlight its importance and versatility in modern technological applications.

2.5.1. Electrochromism and photochromism

Since Deb's discovery in the early 1970s of the electrochromic and photochromic properties of WO_3, substantial research has focused on these effects and the optimization of these materials for large-scale applications. The success of electrochromism is evident in its widespread use in products such as electrochromic automobile mirrors and airplane windows. Electrochromic materials are distinguished by their capacity to reversibly alter their optical properties upon the application of an external potential. In particular, the intercalation of small cations (such as H^+, Na^+, or Li^+) into the material's structure triggers a color change from transparent to blue, which is a defining characteristic of the electrochromic behavior of amorphous WO_3. For instance, the incorporation of protons (H^+) and electrons (e^-) into WO_3 causes a shift from a transparent (bleached) state to a colored state. This process is partially reversible, with a maximum intercalation limit of $x < 0.5$ protons (Mardare & Hassel, 2019a).

$$(WO_3 + H^+ + e^-)_{bleanhed} \leftrightarrow (H_zWO_3)_{clored} \text{(Reaction4)}.$$

To be more precise, the process depends on the localization of electrons at tungsten sites., causing a shift in the oxidation state from W^{6+} to W^{5+}. When photon absorption occurs, these localized electrons may gain sufficient energy to move to an adjacent site. This electron-phonon interaction results in lattice distortion through the formation of polarons. Furthermore, photon-induced polaron hopping leads to photon absorption and subsequent coloration.

Comprehensive reviews on the electrochromic properties of WO_3 are well-documented in existing literature. This section will specifically address the incorporation of WO_3 into devices that leverage its electrochromic characteristics. One notable technological advancement is the development of "smart windows." The layered structure of an electrochromic (EC) device is schematically depicted in (Figure 2.9.) a and b, alongside images of electrochromic windows in the Boeing 787 Dreamliner (c).

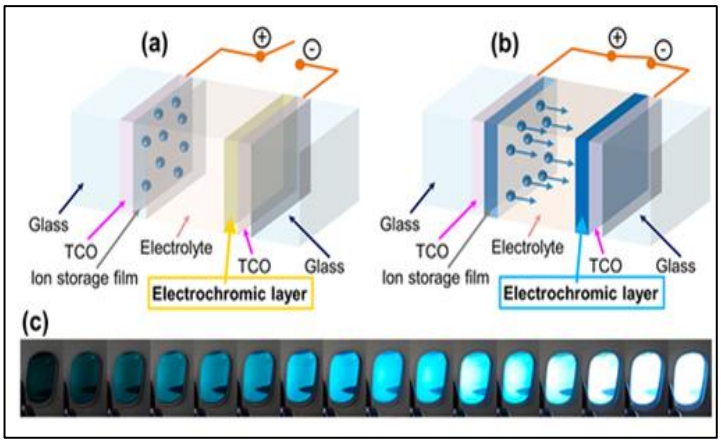

Figure 2.9. Electron hopping in a 1-D chain of atoms

Glass is the most frequently employed substrate material for electrochromic devices; however, flexible plastics that allow for roll-to-roll manufacturing can also be utilized. Glass panes coated with a layer of transparent conducting oxide (TCO) constitute the outer layers of the stack. The most frequently used TCO is Sn-doped In_2O_3 (ITO), although doping with other elements (e.g., Zn or Nb) has shown suitable electrical characteristics. Given the increasing cost and limited availability of indium, alternative transparent conducting oxides (TCOs) like doped-ZnO and doped-SnO_2 have been explored and show promising potential for applications in electrochromic devices. Additionally, very thin, highly conductive metallic layers (Cu, Ag, and Au) or organic compounds (PEDOT) are also being considered.

Between these two glass panes, which have transparent electrodes coated on the inside, The structure comprises three layers: an electrochromic WO_3 thin film, an ion conductor (electrolyte), and an ion storage thin film. When a modest potential difference (less than 5 V DC) is applied between the electrodes, cations from the ion storage layer (e.g., an electrochromic material like NiOH) are transferred through the ion-conducting thin film. The ion conducting layer can be Ta oxide for H^+ transport or polymeric electrolytes like PEO-PEGMA: Li for Li^+, depending on the type of cation being used. When cations enter the WO_3 active layer, The cations combine with electrons from the external circuit to generate coloration (Reaction 4). During ion removal, a reverse process occurs in the ion storage layer, which intensifies the overall coloration effect. The window becomes transparent again when the opposite potential is applied. Various levels of coloration can be achieved using intermediate voltages,

as electrochromic materials can maintain their coloration under open-circuit conditions.

The research and development of electrochromic materials for everyday use have led to many successful commercial applications. Major producers of WO_3-based smart windows include EControl-Glas GmbH & Co. KG (Germany), GESIMAT GmbH (Germany), ChromoGenics AB (Sweden), and SAGE Electrochromics, Inc. (USA). An innovative use of WO_3 electrochromism was developed by Marques, who created a colorimetric sensor using ordinary office paper infused with WO_3 nanoparticles. This sensor detected the electrochemically active bacterium Geobacter sulfurreducens through a bioelectrochromic reaction, where the bacterium's electron transfer to WO_3 caused a color change.

Photochromism, which involves a reversible color change due to photoirradiation, is similar to electrochromism. The photochromic behavior of WO_3 has been thoroughly investigated, but it remains not entirely comprehended. As a semiconductor, tungsten oxide generates electron-hole pairs under light irradiation, which can alter optical absorption and cause a color shift from bleached to blue. Photogenerated holes in the conduction band interact with adsorbed surface humidity to produce H^+, forming tungsten bronze ($HxWO_3$). Optical transitions and electron transfer between tungsten ions in different valence states occur simultaneously. Usually, heat treatment is required to eliminate structural defects and restore the material to its bleached state; however, emerging techniques like surface nanostructuring are being developed to address this challenge.

Photochromic materials are expected to find commercial applications, such as in photochromic pigments or nanoinks, though their use has not been extensively explored yet (Parreira et al., 2006), (Mardare & Hassel, 2019a), (Sato et al., 2008).

2.6. Silicon Dioxide-SiO_2

Silicon dioxide (SiO_2), commonly known as silica, is a fundamental component in various natural and synthetic materials. In silica, silicon atoms typically exhibit tetrahedral coordination, being surrounded by four oxygen atoms. This tetrahedral

configuration is common to most forms of silicon dioxide, leading to a wide variety of structures and applications. Forms of Silica:

Silica exists in nature in two primary forms: crystalline and amorphous. The crystalline form is subdivided into three main types: quartz, tridymite, and cristobalite. These crystalline forms remain stable across various temperature ranges and can be further subdivided. For instance, quartz can exist as alpha quartz at lower temperatures and transforms into beta quartz at 573°C. When heated to 870°C, tridymite forms, and at 1470°C, cristobalite emerges. The melting point of silica is notably high at 1610°C, which exceeds that of metals like iron, copper, and aluminum. This high melting point makes silica an excellent material for producing molds and cores in metal casting processes (Zou et al., 2013).

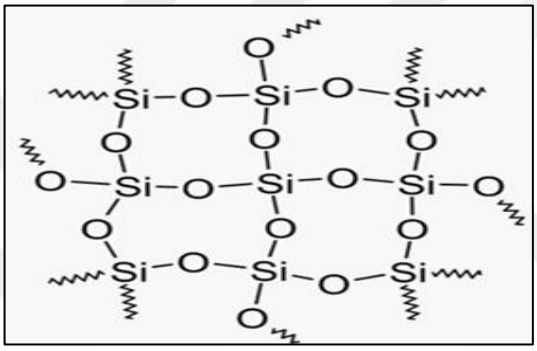

Figure 2.10. Structure of SiO2

Crystalline Silica: Quartz is the most prevalent natural form of crystalline silica. Its crystal structure consists of a three-dimensional network of oxygen atoms forming tetrahedra, each centered on a silicon atom as showing in (Figure 2.11). These tetrahedra are linked by shared oxygen atoms, resulting in a strong crystal lattice. Quartz crystals can be colorless or white, though impurities like iron can impart various colors. Quartz's hardness, resulting from the strong atomic bonds, allows it to scratch glass and renders it relatively inert to dilute acids. These properties make quartz valuable in numerous industrial applications, including glass production, where its vitreous luster and transparency are highly prized(Khalil et al., 2014),(Lin & Heaney, 2017).

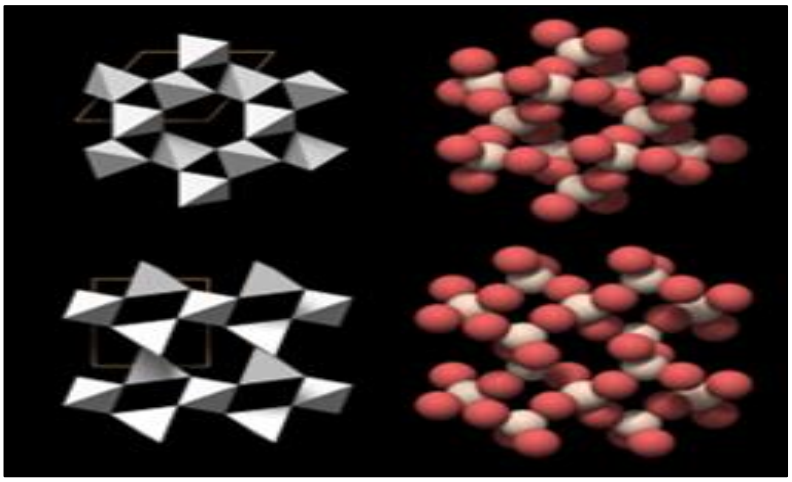

Figure 2.11. Structure of Quartz

Amorphous Silica: Amorphous silica does not have the long-range order found in crystalline forms, which makes it more reactive with alkalis at room temperature. In contrast, crystalline silicon dioxide dissolves much more slowly in hot alkaline solutions. This distinction in reactivity is crucial for various industrial processes that utilize silica in different forms. Industrial Applications: Silica's adaptability extends to its synthetic variants, such as fused silica, fumed silica, silica gel, and aerogels. These materials find applications in construction, microelectronics, and the food industry. Silica's industrial applications have a long history, originating from metallurgical processes and glass production approximately three to five thousand years BC. Over the centuries, silica has continued to play a crucial role in advancing human technology, especially in the glass, foundry, and ceramic industries. In modern times, silica plays a pivotal role in the information technology revolution. It is used in the manufacturing of plastics for computer mice and as a raw material for silicon chips. Quartz grains, depending on their formation process, can exhibit various shapes, from sharp and angular to partially rounded. Foundry and filtration applications benefit from partially rounded grains for optimal performance(Zou et al., 2013). The properties of Silicon dioxide are summarized in Table2.2.

Table 2.2. Properties of Silicon dioxide.

Property	Silicon Dioxide (SiO_2)
Crystal Structure	Amorphous or crystalline (quartz, cristobalite)
Band Gap	8.9 eV (insulator)
Optical Properties	High transparency in UV and visible light range
Photocatalysis	Inert, does not exhibit photocatalytic activity
Density	~2.65 g/cm³
Hardness	High hardness, excellent wear resistance
Thermal Stability	Stable up to 1,600°C
Corrosion Resistance	Excellent chemical stability, corrosion resistance
Electrochromism	No electrochromism
Thermochromism	No thermochromism
Electrical Properties	Electrical insulator
Mechanical Properties	High mechanical strength, durable, scratch-resistant
Chemical Activity	Chemically inert

Photochromic compounds are intriguing molecules that alter their color in response to light. They find applications in research labs and factories alike, most notably in eyeglass lenses, but also have promise for data storage, optical switches, sensing, rewritable optical media, and other applications. Photochromism could also find success in textiles, enabling "smart" fabrics and clothing that can sense environmental changes, absorb UV radiation, and display dramatic color transitions.

Photochromic compounds are incorporated into textiles either by spinning them into fibers with conventional dyeing techniques, or by surface-coating the textiles with microcapsules. But the inflexible polymer matrix surrounding the chromophore can impede the coloration/bleaching process, leading to poor switching speeds and stability. Coating photochromic microcapsules onto fabrics can also impart an unpleasantly rough texture to the final apparel, detracting from wearer comfort (Brinker & Scherer, 1990). (Figure 2.12) demonstrates the photochromic response of

a molecule when exposed to UV light. The structure on the left depicts its original form, while the structure on the right reveals the modified state after absorbing light energy (hv). This reversible transformation results from a molecular rearrangement, causing a change in optical properties. Photochromic molecules like these are often incorporated into silicon dioxide coatings to create smart materials that respond to light, making them ideal for applications such as self-adjusting windows and advanced optical systems.

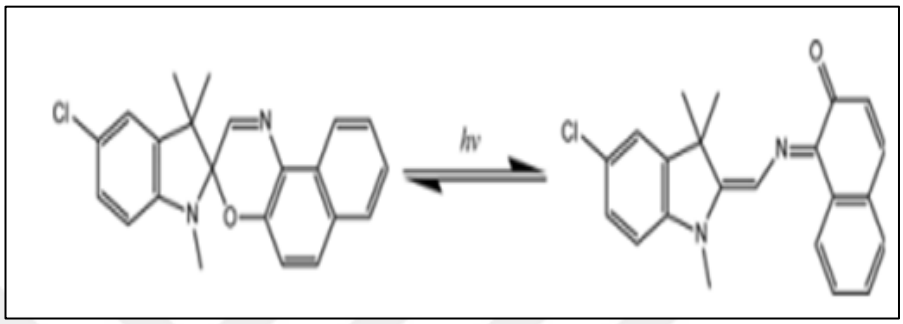

Figure 2.12. The photochromic effect

A sol-gel technique has been effectively utilized to embed dyestuffs in hybrid organic-inorganic silica matrices, resulting in the development of functional coatings for applications in photonics and sensing. Silica is a very suitable host for photochromic molecules because its network possesses a large number of “nano-sized” tiny pores, allowing for sufficient free volume for the molecules to facilitate the photochromic transition (Tong Cheng et al., 2007).

If a redox reaction can occur in the presence of an external potential, the material may exhibit reversible optical properties upon application of an external potential. This property is called electrochromism. Electrochromic materials have garnered significant interest recently due to their broad potential applications, including in electrochromic 'smart' windows, anti-glare rearview mirrors, displays, and camouflage. These materials can be categorized into four types: metal oxides, metal coordination complexes, metal hexacyano metallates, and conjugated conducting polymers. Transition metal oxide films (e.g. tungsten or nickel oxide) were the first materials to be studied for electrochromism in the early research of electrochromism because of their high optical modulation. But nowadays these materials are usually limited by incompatibility issues, complicated processing, monochromatic coloration

changes and slow response speeds. Conjugated conducting polymers have received much attention for use in electrochromic devices in recent years because of their attractive properties, such as fast switching times, easy processability, high contrast and multicolour capabilities. Few studies have been reported on silicon dioxide (SiO_2) coatings for photochromic applications. Although an extensive study has not been completed, chemical dispersion polymerization method was employed to synthesize SiO_2/PANI nanocomposites.

Figure (2.13.) schematic representation of the synthesis and testing process for SiO_2/PEDOT nanocomposites. The procedure begins with the dispersion of EDOT in an EDOT-HCl solution, followed by the addition of SiO_2 nanoparticles, which absorb EDOT monomers. In situ polymerization occurs, resulting in the formation of SiO_2/PEDOT nanocomposites. These nanocomposites are then fabricated into thin films and assembled into an electrochromic device (ECD-SiPD). Finally, the electrochemical performance of the film is evaluated through testing. The as-prepared SiO_2/PANI film exhibits high electrochromic stability, this further supports the notion that incorporating SiO2 can enhance the electrochromic performance of conductive polymers. To the best of our knowledge, a comprehensive study on the electrochemical and electrochromic properties of SiO_2/PEDOT nanocomposites has not yet been conducted. (Zhang et al., 2019).

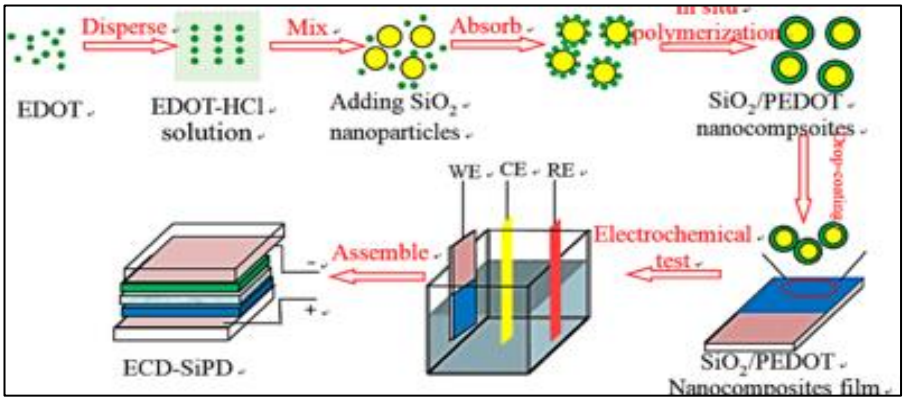

Figure 2.13. Schematic diagram of fabricated electrochromic device based on SiO_2/PEDOT core/shell nano-composite film

2.7. Silica Coating

Monodisperse spherical silica nanoparticles were prepared by the sol-gel processing of silicon alkoxides in basic aqueous solutions containing alcohols (methanol, ethanol, or isopropanol) by Stöber and co-workers in the late 1960s (Stöber et al., 1968). Before silica coating, some bifunctional molecules should be used in aqueous solutions to strongly coordinate on the surface-protected nanoparticles in alcoholic solutions via surface coordination or electrostatic attraction. The hydrolysis and condensation of tetraethyl orthosilicate (TEOS) occur via reactive hydroxyl groups on the nanoparticle interface. Silica coating has attracted much attention due to its outstanding properties, such as rich surface chemistry, high biocompatibility, tunable porosity, and superb transparency, in combination with metal nanoparticles (Vrancken et al., 1995). The surface chemistries and interface properties of metal nanoparticles should be well exploited to design and construct robust interfaces and good surface coating.

2.7.2. Silica coating of metal

Silica coating of metal nanoparticles is carried out by using some bifunctional molecules in aqueous solutions to strongly coordinate on the surface-protected nanoparticles in alcoholic solutions via surface coordination or electrostatic attraction. The hydrolysis and condensation of TEOS occur via reactive hydroxyl groups on the nanoparticle interface (Stöber et al., 1968). Silica coating has attracted much attention due to its outstanding properties, such as rich surface chemistry, high biocompatibility, tunable porosity, and superb transparency, in combination with metal nanoparticles (Vrancken et al., 1995).

2.7.3. . Silica coating by sol-gel

SiO_2 has a large number of physical properties, which are favorable for thin-film applications. SiO_2 films are applicable to a variety of protective and anti-reflective coating because of their excellent permeability and chemical stability in the visible region. SiO_2 films are especially useful for different microelectronic structures because of their dielectric nature. Sol-gel-derived silica films have many unusual

properties, including high porosity, controllable microstructure, refractive index, high laser damage threshold, and good transmittance in the visible region.

2.7.4. Uses of silica

Silicon dioxide (SiO_2), or silica as it is often known, occurs mainly as sand. Crystalline silica is a natural ore which can be used in various industries. Chemical inertness or the incapacity of silica to react easily with reagents is the principal property associated with its numerous applications. Silica's physical properties, including its high melting point and particulate form, determine its suitability for various applications. The methods of forming and processing silica granules establish the particle shape. Mining and processing convert quartzite or sand to.

2.7.5. Industrial and metallurgy

Water Filtration and Purification: Silica filters and purifies water by reason of its chemical inertness and stability. Filler Sand: Silica sand serves as filler material in various industrial applications. Foundry Sand: Silica is utilized in foundries for molding and casting due to its high melting point. Specialized Flooring Solutions: Silica used in flooring solutions which demand durability and resistance. Refractories: Silica used in refractory materials due to its high melting point. Glass Manufacturing: Silica is major raw material in glass production. Paints and Wall Coatings: Silica used to enhance properties of paints and coatings. Silica Flux: It is used in metallurgy as a flux to remove impurities.

2.7.6. Construction and mining

- Tile Manufacturing: Silica is a major component in tile production.
- Grouts, Adhesives, Epoxy and Specialized Cements: Silica is used to enhance the properties of construction materials.
- Drilling: Silica used in drilling operations because of its abrasiveness and stability.

2.8. Sol-Gel Coating Techniques

- Sol-Gel Coating Techniques:

The sol-gel process is a sophisticated and effective method for preparing oxide materials, allowing for precise control over both composition and structure (Brinker & Scherer, 1990). It involves the hydrolysis and condensation of metal alkoxides or salts in solution, followed by the gelling of the resulting sol. This process can be utilized to deposit thin films onto various substrates. The sol-gel routes have wide applications since the resulting materials properties can be tailored for different applications such as electronics, construction, automotive, energy, and protection coatings(Belleville, 2010).

- Underlying Processes and Chemistry:

Hydrolysis of metal alkoxides or salts in presence of water generates hydroxyl groups that then condense to form an oxide network. The cross--linking of the network is essential for the formation of the film and the sol (a mixture of solid particles suspended in a liquid) gels. The gel is then dried and heated to eliminate the residual solvents and to improve the structural properties. The flowing steps are depicted in (Figure 2.14.).

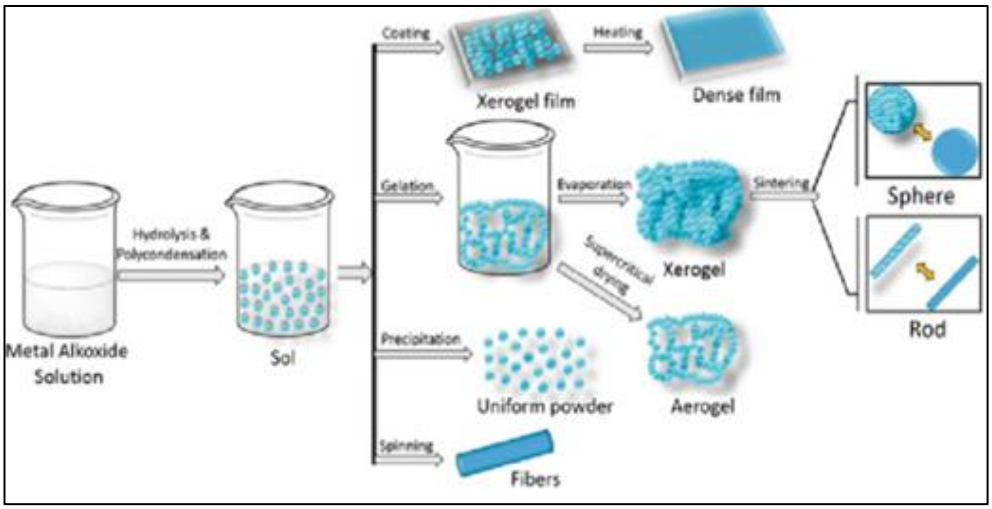

Figure 2.14. Schematic representation of Sol-Gel processing

- Industrial Applications:

Sol-gel coatings find applications in electronics where thin films are used to improve the properties and device performance. In construction materials, sol-gel products are added as concrete additives and as water-repellent treatments. Additionally, they play a vital role in electrochemical devices, such as sensors and fuel cells, offering both corrosion protection and functional benefits. Sol-gel coatings are also employed in the automotive industry for applications like paints and glass coatings.

- Pros and Cons:

The major benefits of the sol-gel technique are the easy control of composition, the ability to utilize temperature-sensitive materials and the lower cost compared to alternative preparation methods (Brinker et al., 1991). The process allows the deposition of homogeneous coatings with controlled properties such as thickness, refraction, absorption, permeability, porosity, functional groups and electrical conductivity. On the other hand, sol-gel coatings usually lack mechanical strength and some materials may be brittle. Further, the process has to be controlled since it is highly sensitive to humidity and temperature. These limitations imply that scaling up to industrial or production scale is usually not easily accomplished.

- Various Coating Techniques:

From the sol-gel process different coating techniques have been developed with their respective benefits:

- Dip Coating:

Dip coating is also referred to as slurry coating or vacuum slurry coating.

This method is used for structures of functional layers. In this method, slurry is used in the production process. It is produced from slurry, ceramic powder, solvent and binder products. In the dip coating process, the support layer is immersed in a slurry. The jar is then lowered, causing a film of the slurry to adhere to the support. After the coated slurry dries at room temperature, the supported layer is sintered along with the newly dip-coated layer. This method can produce layers ranging from a few microns

to several hundred microns in thickness. (Figure 2.15.) shows the illustration of dip coating steps (Brinker et al., 1991).

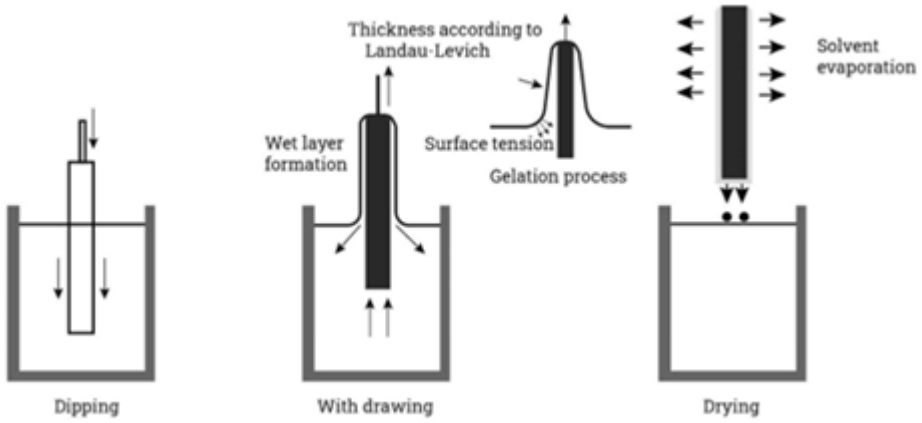

Figure 2.15. Dip coating process

- Spin Coating:

Liquid coatings are spread over rotating substrates by centrifugal force. This technique is used for the production of thin films with a thickness that can be easily controlled.

- Spray Coating:

Sol-gel solutions are rapidly and efficiently applied using this method. It is well-suited for processing large areas and for continuous applications. Advancements in both existing and novel sol-gel techniques will expand their range of applications and enhance the properties of the materials. An important task is the scaling up to industrial or production scale. Moreover, the preparation of materials with improved flexibility, adhesion to substrates and resistance against detergents and cleaning agents should be investigated. Exploring new potential applications in high-value fields such as nanotechnology and biomedicine represents another key objective for the future.

To conclude, sol-gel coating techniques are fundamental procedures in materials science with versatile applications in different industrial fields. As engineers and researchers, it is essential to comprehend and refine these coating methods to fully realize their potential and create smart materials with tailored properties, paving the way for innovative solutions across a wide range of industries.

3. EXPERIMENTAL STUDIES

3.1. Solution Preparation

The preparation of the coating solution through the sol-gel method involves a structured approach to achieve a stable and homogeneous mixture. This process begins with the careful transfer of components into a container, adhering to specific molar ratios: TEOS (tetraethyl orthosilicate) at 1, ethanol at 45, glycerol at 1, and ammonium hydroxide (N_4OH) at 2. TEOS serves as the precursor for the silica network, while ethanol acts as a solvent to dilute the TEOS, facilitating the hydrolysis and condensation reactions. Glycerol, a polyol, enhances the solution's viscosity, promoting uniform distribution of tungsten chloride (WCl_4) particles. Following the initial mixing using a magnetic stirrer set at 500 rpm until homogeneity is achieved, approximately 2 grams of WCl_4 powder are introduced, which is essential for enhancing the functional properties of the resulting thin films. The mixture is subsequently stirred at a heightened speed of 700 rpm for 20 additional minutes to ensure complete dissolution of the tungsten chloride and promote uniformity throughout the solution. In (Figure 3.1.) Daihan Scientific MaXtir™ 500S magnetic stirrer and Metler Toledo S210-U model benchtop pH meter illustrates the equipment used in the preparation of preparing tungsten oxide – silicon oxide composite sol can be seen.

The pH of the resulting solution is carefully adjusted to approximately 10, crucial for controlling the hydrolysis and condensation rates of TEOS. The alkaline conditions favor the condensation reaction, encouraging the establishment of a more cross-linked silica network within the coating. After achieving a consistent mixture, the solution is allowed to age for one week, which is vital for transforming the solution into a sol. This aging process promotes essential chemical interactions and structural developments, culminating in a stable and well-formed sol, ready for various applications, particularly in thin-film deposition where precise control over the composition and morphology is required.

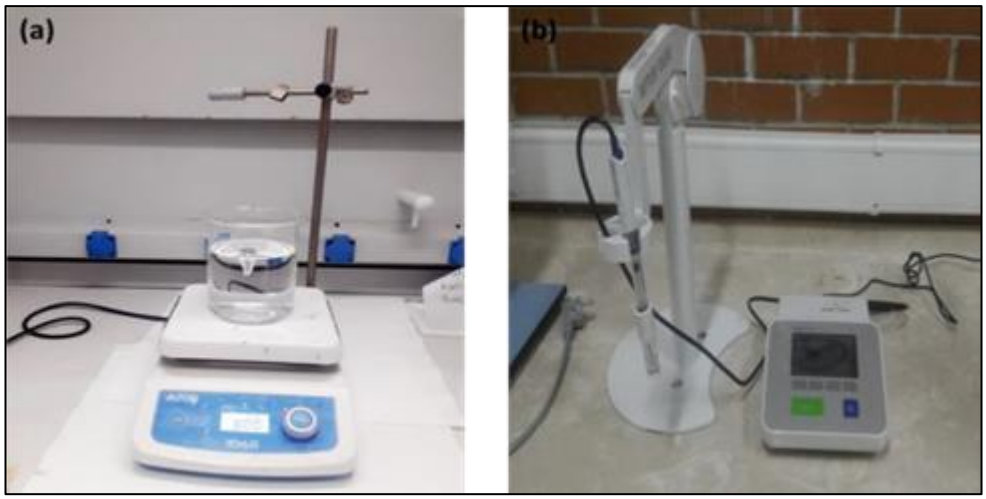

Figure 3.1. (a) magnetic stirrer (b) benchtop pH meter

3.2. Substrate Preparation

Soda-lime glass substrates were utilized for thin film deposition in this study, chosen for their abundance, affordability, good transparency, and favorable mechanical properties. However, ensuring surface cleanliness is paramount for successful thin film deposition, as impurities can significantly interfere with adhesion and the uniformity of the film. To achieve a pristine substrate surface, a rigorous cleaning protocol was employed, involving a thorough ultrasonic bath treatment. The cleaning process was conducted in sequential stages: the substrates were immersed in acetone, ethanol, and deionized water, each treatment lasting 10 to 15 minutes.

Acetone, recognized as an effective organic solvent, was utilized to dissolve oils, greases, and other organic contaminants from the glass surfaces. Ethanol was included in the protocol due to its rapid evaporation and ability to dissolve organic residues without leaving behind any traces. The ultrasonic cleaning method leverages high-frequency sound waves to generate cavitation bubbles, which effectively scrub both organic and inorganic particles from the substrate surface, enhancing the overall cleaning efficacy.This application of mechanical energy ensures that contaminants are removed at the micro-level, resulting in a clean and prepared substrate suitable for thin film deposition. The effectiveness of ultrasonic cleaning has been well-documented in numerous surface treatment studies and is recognized as a standard procedure in

substrate preparation for thin-film applications. (Figure 3.2.) shows an ultrasonic cleaning bath.

Figure 3.2. Cleaning of the substrates

3.3. Dip- Coating Technique and Film Formation

The coating was applied using the dip-coating machine (Teknosem TDC-10), where the soda-lime glass substrates were immersed into the sol and withdrawn at a controlled speed of 60 mm/min. Dip-coating is advantageous for producing uniform thin films because it allows control over the film thickness, depending on the withdrawal speed, viscosity of the solution, and environmental conditions such as humidity and temperature (Brinker & Scherer, 1990), as the substrate is withdrawn, a thin layer of the sol adheres to the surface due to surface tension and viscous forces. The uniformity of the coating is influenced by the speed of withdrawal, which in this case was set at 60 mm/min. At this speed, a fine balance is achieved between film thickness and coating homogeneity. Faster speeds result in thicker films, whereas slower speeds can lead to uneven deposition due to gravitational effects.

After withdrawal, the films were left to air-dry. This drying process allows the solvent to evaporate and initiates the transition of the sol into a gel-like state, forming a solid, thin film on the substrate, (Figure 3.3.) shows the dip coating machine used in this study.

Figure 3.3. Dip coating machine

3.4. Annealing of the Coatings

The annealing process was a critical step in enhancing the structural, mechanical, and functional properties of the thin-film coatings prepared in this study. The samples were annealed to 300 and 500°C with 5 °C/min heating and cooling rates for 1 hour duration. Annealing induce significant structural changes, including the removal of residual organic materials and the densification of the silica network. At these temperatures, the cross-linking within the silica matrix increases, promoting the mechanical stability of the film.

Once the cooling period was complete, the samples were removed from the oven and allowed to reach room temperature naturally. Allowing the sample to equilibrate with the ambient environment without forced cooling further reduces the chances of stress-induced defects.

3.5. Characterization Of The Coatings

The microstructural features was examined using a scanning electron microscope (JEOL JSM-7600F SEM). The wetting properties were measured by Thetalite 101 Biolin Scientific equipment. The optical transmittance properties of the coatings were evaluated using a UV-vis spectrophotometer (Jasco V-530 UV/VIS Spectrophotometer). Photocatalytic activity measurements were realized by observing the decolorization of the methylene blue (MB) with visible light irradiation.

3.6. SEM Analysis

The microstructural properties of the WS1 and WS2 samples were investigated using Scanning Electron Microscopy (SEM). The SEM images in (Figure 3.4.) reveal that both specimens have uniformly distributed nanoparticle structure.

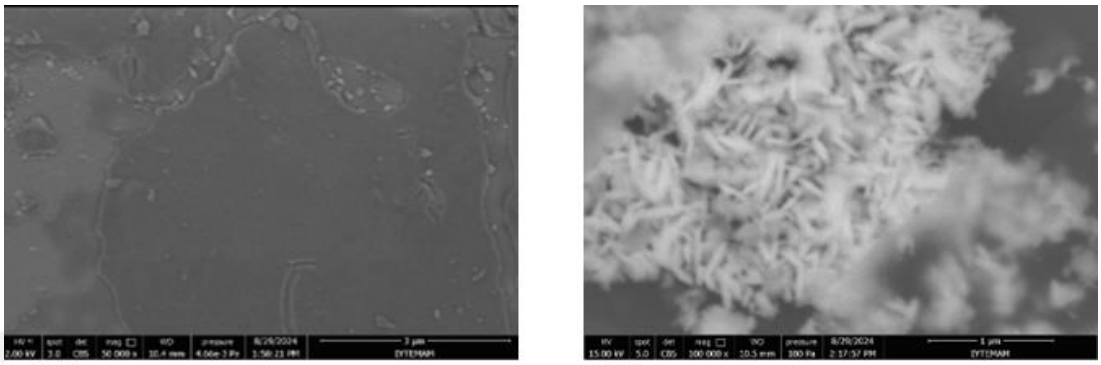

Figure 3.4. SEM micrographs of WS1 and WS2

3.7. Photocatalytic Activity

The photocatalytic efficiency of WS1 and WS2 coatings was evaluated based on their ability to degrade methylene blue (MB) under simulated daylight. Figure (3.5.) presents the results, including the degradation curves over time (Figure 3.5.a) and the photodegradation efficiency percentages (Figure 3.5.b).

As seen in (Figure 3.5a), WS2 exhibits superior photocatalytic performance compared to WS1. Specifically, WS2 achieved a degradation efficiency of 70.00% after 7 hours, whereas WS1 showed a lower degradation efficiency of 66.42%. The uncoated glass substrate (reference) demonstrated an efficiency of only 60.31%, confirming that the photocatalytic activity enhanced by the coatings.

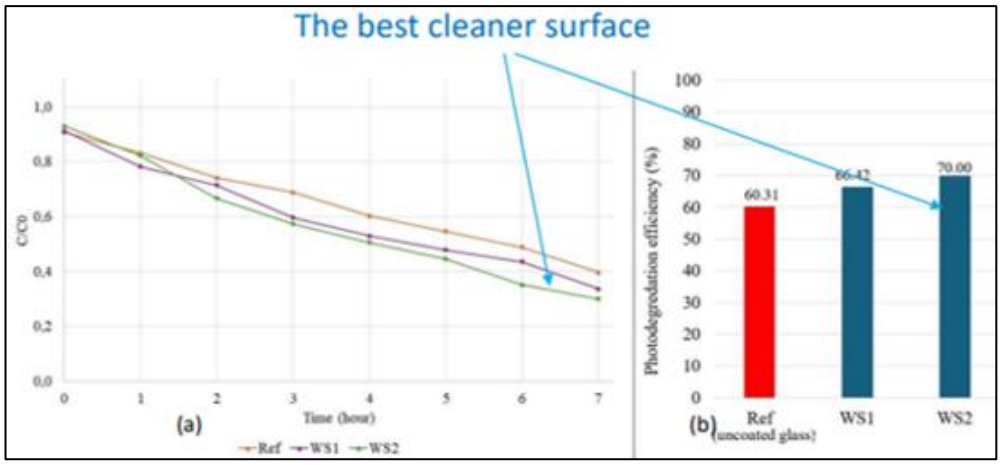

Figure 3.5. (a) Photodegradation curves, and (b) photodegradation efficiency of WS1, WS2, and uncoated glass

The photocatalytic mechanism of tungsten oxide – silicon dioxide coatings is primarily driven by the absorption of visible light by the tungsten oxide component. When illuminated, tungsten oxide absorbs photons with energy greater than its bandgap, exciting electrons from the valence band to the conduction band and generating electron-hole pairs. These charge carriers migrate to the surface of the nanocomposite film, where they interact with water and oxygen molecules absorbed on the surface. This interaction produces reactive oxygen species (ROS), such as hydroxyl radicals and superoxide ions which are highly reactive and capable of breaking down organic pollutants like methylene blue into harmless byproducts.

3.8. Wettability

The wettability of the synthesized coatings was evaluated using contact angle measurements. The results, presented in Figure (3.6.) reveal that both WS1 and WS2 exhibit hydrophilic behavior, with WS2 displaying a more pronounced hydrophilic nature due to its lower contact angle.

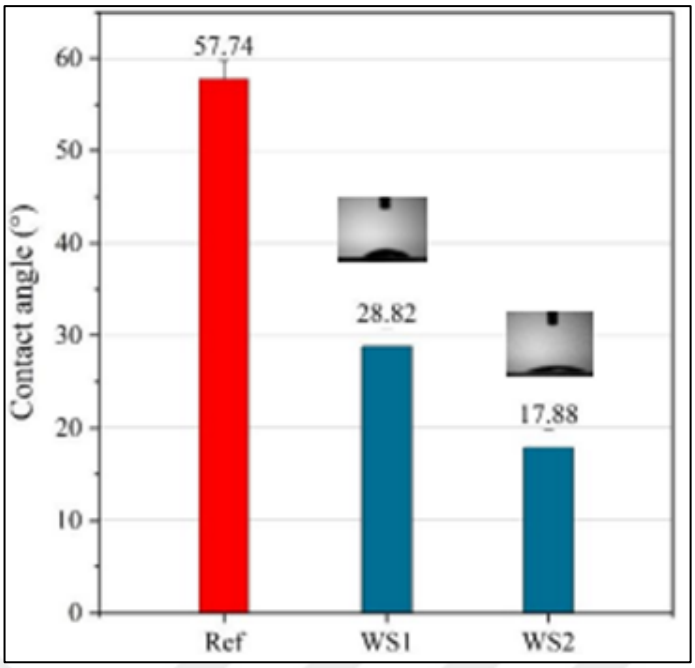

Figure 3.6. Contact angle of WS1, WS2, and glass

The contact angle of WS1 was measured at 28°, while WS2 had a significantly lower contact angle of 17°, indicating better wettability. In contrast, the uncoated glass exhibited a much higher contact angle.

This enhanced hydrophilicity in WS2 makes it a good candidate for photocatalytic applications, where surfaces need to allow water to spread and carry away contaminants. The combination of hydrophilicity and photocatalytic activity allows the nanocomposite coatings to break down organic pollutants and remove them with water flow, supporting their use in environments where cleanliness is critical.surface.

3.9. Optical Properties

The optical transmittance of WS1 and WS2 was measured using UV-Vis spectrophotometry, and the results are shown in (Figure 3.7.) both samples displayed high transmittance in the visible light range of around 90%, comparable to the uncoated glass, indicating that the coatings allow substantial light to pass through. These properties help reduce light scattering within the film, thereby allowing more

photons to pass through the material hence more suitable for photocatalytic applications.

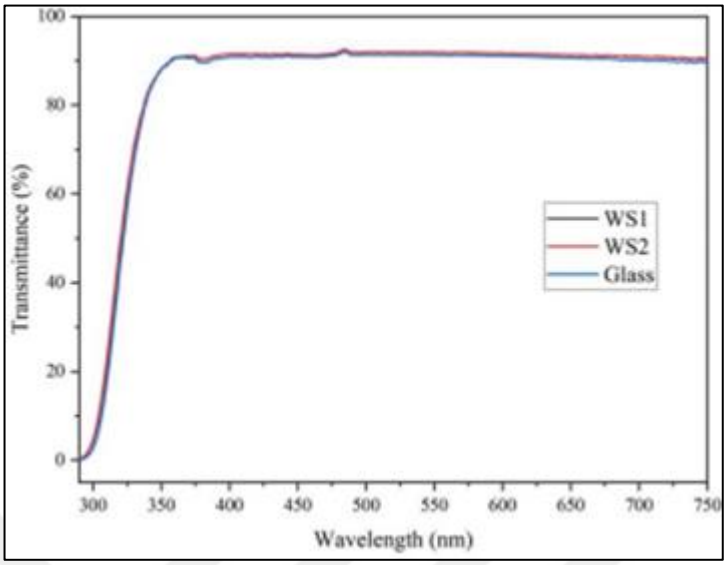

Figure 3.7. Transmittance % of WS1, WS2, and glass

4. CONCLUSIONS

In this sudy, the synthesis of tungsten oxide-silicon dioxide nanocomposite coatings via sol-gel dip coating were succesfully realized. Following conclusions were drawn;

- According to the microstructural analysis realized by SEM, both coatings were homogenously nanostructured.
- Optical analyses demonstrated that both coatings annealed at 300 °C and 500 °C have high transmittance values of about 90% thus they are completely transparent.
- As a result of contact angle measurements, 28° and 17° were found for WS1 annealed at 300 °C and WS2 annealed at 500 °C respectively, demonstrating that they are highly hydrophilic.
- According to the photocatalytic activity measurements realized under artifical daylight, WS1 demonstrated 66% and WS2 70% of MB degredation efficiencies demonstrating that they are good candidates for photocatalytic applications.
- Overall, WS2 was identified as the more effective coating for applications requiring high transparency, photocatalytic activity, and self-cleaning properties. The findings from this study suggest that tungsten oxide-silicon dioxide nanocomposite coatings hold significant potential for use in environmental and energy-efficient applications, such as solar energy devices, smart windows, and photocatalytic surface treatments.

REFERENCES

Ahmadi, S., Rabiee, N., Bagherzadeh, M., Elmi, F., Fatahi, Y., Farjadian, F., Baheiraei, N., Nasseri, B., Rabiee, M., Dastjerd, N. T., Valibeik, A., Karimi, M., & Hamblin, M. R. (2020). Stimulus-responsive sequential release systems for drug and gene delivery. *Nano Today*, *34*, 100914. https://doi.org/https://doi.org/10.1016/j.nantod.2020.100914

Arendt, M. F., & Wilkinson, D. S. (2000). A nonperturbative density functional analysis for nonuniform Lennard-Jones fluid. *The Journal of Chemical Physics*, *113*(19), 8717–8718. https://doi.org/10.1063/1.1318775

Bauer, M., Tolle, J., Bungay, C., Chizmeshya, A., Smith, D., Menendez, J., & Kouvetakis, J. (2003). Tunable band structure in diamond–cubic tin–germanium alloys grown on silicon substrates. *Solid State Communications*, *127*, 355–359. https://doi.org/10.1016/S0038-1098(03)00446-0

Belleville, P. (2010). Functional coatings: The sol-gel approach. *Comptes Rendus Chimie*, *13*(1–2), 97–105. https://doi.org/10.1016/j.crci.2009.12.005

Besozzi, E., Dellasega, D., Russo, V., Conti, C., Passoni, M., & Beghi, M. G. (2019a). Thermomechanical properties of amorphous metallic tungsten-oxygen and tungsten-oxide coatings. *Materials and Design*, *165*. https://doi.org/10.1016/j.matdes.2018.107565

Besozzi, E., Dellasega, D., Russo, V., Conti, C., Passoni, M., & Beghi, M. G. (2019b). Thermomechanical properties of amorphous metallic tungsten-oxygen and tungsten-oxide coatings. *Materials and Design*, *165*. https://doi.org/10.1016/j.matdes.2018.107565

Brinker, C. J., Frye, G. C., Hurd, A. J., & Ashley, C. S. (1991). Fundamentals of sol-gel dip coating. *Thin Solid Films*, *201*(1), 97–108. https://doi.org/10.1016/0040-6090(91)90158-T

Brinker, C. J., & Scherer, G. W. (1990). *The Physics and Chemistry of Sol-Gel Processing*.

Cheng, T., Lin, T., Brady, R., & Wang, X. (2008). Fast response photochromic textiles from hybrid silica surface coating. *Fibers and Polymers*, *9*(3), 301–306. https://doi.org/10.1007/s12221-008-0048-7

Claes G. Granqvist. (1995). *Handbook of Inorganic Electrochromic Materials*.

Clarke, S. (2008). Chapter 1 - Fundamentals of chemistry. In S. Clarke (Ed.), *Essential Chemistry for Aromatherapy (Second Edition)* (pp. 7–24). Churchill Livingstone. https://doi.org/https://doi.org/10.1016/B978-0-443-10403-9.00001-7

Granqvist, C. G. (1999). Progress in electrochromics: tungsten oxide revisited. *Electrochimica Acta*, *44*(18), 3005–3015. https://doi.org/10.1016/S0013-4686(99)00016-X

Granqvist, C. G., Avendaño, E., & Azens, A. (2003). Electrochromic coatings and devices: survey of some recent advances. *Thin Solid Films*, *442*(1–2), 201–211. https://doi.org/10.1016/S0040-6090(03)00983-0

Hu, J., Zhang, J., Li, H., Chen, Y., & Wang, C. (2017). A promising approach for the recovery of high value-added metals from spent lithium-ion batteries. *Journal of Power Sources*, *351*, 192–199. https://doi.org/10.1016/j.jpowsour.2017.03.093

Iwai, D., Takeda, S., Hino, N., & Sato, K. (2014). Projection screen reflectance control for high contrast display using photochromic compounds and UV LEDs. *Optics Express*, *22*(11), 13492–13506. https://doi.org/10.1364/OE.22.013492

Jabur, M., & Al-Fatlawi, K. (n.d.). *Institute of Graduate Studies Electrical And Computer Engineering CONTROL AND MANAGEMENT OF SOLAR CHARGER USING MICROGRIDS AND PHOTOVOLTAIC CELLS*.

Jeon, M., Joo, K.-N., Kim, T., Kim, S., & Youn, C.-H. (2022). FleX: A Flex Interconnected HPC System With Stochastic Load Balancing Scheme. *IEEE Access*, *10*, 37164–37180. https://doi.org/10.1109/ACCESS.2022.3163542

Khalil, Z. Bin, Yamashita, M., Kuno, Y., & Hattori, T. (2014). Energy Absorption Performance of Press-formed Shell. *Procedia Engineering*, *81*, 951–956. https://doi.org/10.1016/j.proeng.2014.10.123

Kim, Y.-G., Tatami, J., Komeya, K., & Kim, D. K. (2006). Effect of the microstructure of Si3N4 on the adhesion strength of TiN film on Si3N4. *Thin Solid Films*, *510*(1–2), 222–228. https://doi.org/10.1016/j.tsf.2005.12.304

Kosinski, J. A. (2005). Nanotechnology evolution in piezoelectric resonator sensors. *Proc.SPIE*, *5592*, 282–295. https://doi.org/10.1117/12.580329

Lin, X., & Heaney, P. J. (2017). Causes of Iridescence in Natural Quartz. *Gems & Gemology*, *53*(1), 68–81. https://doi.org/10.5741/GEMS.53.1.68

Linderälv, C. (n.d.). *Structural and thermodynamical properties of tungsten oxides from first-principles calculations*.

Livage, J., Henry, M., & Sanchez, C. (1988). Sol-gel chemistry of transition metal oxides. *Progress in Solid State Chemistry*, *18*(4), 259–341. https://doi.org/10.1016/0079-6786(88)90005-2

Louzguine, D. V, & Inoue, A. (1999). Multicomponent metastable phase formed by crystallization of Ti–Ni–Cu–Sn–Zr amorphous alloy. *Journal of Materials Research*, *14*(11), 4426–4430. https://doi.org/10.1557/JMR.1999.0599

Mardare, C. C., & Hassel, A. W. (2019a). Review on the Versatility of Tungsten Oxide Coatings. *Physica Status Solidi (A) Applications and Materials Science*, *216*(12). https://doi.org/10.1002/pssa.201900047

Mardare, C. C., & Hassel, A. W. (2019b). Review on the Versatility of Tungsten Oxide Coatings. *Physica Status Solidi (a)*, *216*(12), 1900047. https://doi.org/https://doi.org/10.1002/pssa.201900047

Mardare, C. C., & Hassel, A. W. (2019c). Review on the Versatility of Tungsten Oxide Coatings. *Physica Status Solidi (a)*, *216*(12), 1900047. https://doi.org/https://doi.org/10.1002/pssa.201900047

Niklasson, G. A., Berggren, L., & Larsson, A.-L. (2004). Electrochromic tungsten oxide: the role of defects. *Solar Energy Materials and Solar Cells*, *84*(1–4), 315–328. https://doi.org/10.1016/j.solmat.2004.01.045

Parreira, N. M. G., Carvalho, N. J. M., & Cavaleiro, A. (2006). Synthesis, structural and mechanical characterization of sputtered tungsten oxide coatings. *Thin Solid Films*, *510*(1–2), 191–196. https://doi.org/10.1016/j.tsf.2005.12.299

Sato, R., Kawamura, N., & Tokumaru, H. (2008). The coloration of tungsten-oxide film by oxygen deficiency and its mechanism. *Applied Surface Science*, *254*(23), 7676–7678. https://doi.org/10.1016/j.apsusc.2008.01.161

Späth, B., Lakus-Wollny, K., Fritsche, J., Ferekides, C. S., Klein, A., & Jaegermann, W. (2007). Surface science studies of Cu containing back contacts for CdTe solar cells. *Thin Solid Films*, *515*(15), 6172–6174. https://doi.org/10.1016/j.tsf.2006.12.054

Stöber, W., Fink, A., & Bohn, E. (1968). Controlled growth of monodisperse silica spheres in the micron size range. *Journal of Colloid and Interface Science*, *26*(1), 62–69. https://doi.org/10.1016/0021-9797(68)90272-5

Stuart, B. W. (2016). *Deposition and Characterisation of RF Magnetron Sputtered Phosphate Based Glasses*.

Sudo, S. (1992). Metal-insulator transition and magnetic properties in the NiS2−xSex system. *Journal of Magnetism and Magnetic Materials*, *114*(1), 57–69. https://doi.org/https://doi.org/10.1016/0304-8853(92)90332-I

Thorsten Wagner, S. H. E. M. M. W. H. W. Z. (2000). Metal Oxide Gas Sensors: Sensitivity and Influencing Factors. *Sensors and Actuators B: Chemical*, *65*(1–3), 1–4.

Tong Cheng, Tong Lin, Jian Fang, & Brady, R. (2007). Photochromic Wool Fabrics from a Hybrid Silica Coating. *Textile Research Journal*, *77*(12), 923–928. https://doi.org/10.1177/0040517507083523

Vrancken, K. C., De Coster, L., Van Der Voort, P., Grobet, P. J., & Vansant, E. F. (1995). The Role of Silanols in the Modification of Silica Gel with Aminosilanes. *Journal of Colloid and Interface Science*, *170*(1), 71–77. https://doi.org/10.1006/jcis.1995.1073

W. A. MacDonald. (1992). Electrochromic Coatings: Review of Materials and Applications. *Solar Energy Materials and Solar Cells*, *28*(1–4), 1–19.

Xu, G., Jin, C., Lan, Y., Liu, L., Kong, K., Yang, X., Yue, Z., Li, X., Sun, F., Huang, H., & Zhou, L. (2018). Enhanced conductive core–shell structured Si/Ag@SiOx particles as high performance anode material for lithium ion batteries. *Materials Letters*, *233*, 228–232. https://doi.org/10.1016/j.matlet.2018.09.023

Zhang, S., Hu, F., Chen, S., Du, Z., Peng, H., Yang, F., & Cao, Y. (2019). A Dual-Type Electrochromic Device Based on Complementary Silica/Conducting Polymers Nanocomposite Films for Excellent Cycling Stability. *Journal of Electronic Materials*, *48*(8), 4797–4805. https://doi.org/10.1007/s11664-019-07273-9

Zou, B., Wang, Y., Xu, J., Zhao, S., Fan, X., Hui, Y., Tao, S., Zhou, X., Ma, H., & Cao, X. (2013). Mechanism in reactive plasma spraying synthesis of TiC–TiB_2 composite coating. *Journal of Asian Ceramic Societies*, *1*(4), 322–327. https://doi.org/10.1016/j.jascer.2013.08.005

CURRICULUM VITAE

Personal Information:

Name Surname: M*****d N***R

Nationality: T*****h/ S****n

Date and Place of Birth: 0*/0*/19**, A****o/ S***a

Marital Status: Married

Communication Information:

Phone Number: +90 5** 3** **06

E-mail: m*******r@****l.com

Education

Degree	**University/ School**	**Graduation Year**
Secondary School	School of Computer Technologies/ Syria	2012
Bachelor of Sceince	Mugla Sitki Kocman University/	2020
Master of Science	Mugla Sitki Kocman University/	2023

Professional Experience

Research Assistant | Mugla Sitki Kocman University | Jul 2018 – present

Conducting research on proton-conducting oxides for on-site hydrogen purification as part of the 119M065 project funded by TUBITAK. Investigating composite structures of $BaZr_{0.80}Y_{0.20}O_3$ (BZY) and $SrCe_{0.95}Yb_{0.05}O_3$ (SCY) using a combinatorial approach. Depositing BZY-SCY oxides via magnetron sputtering to produce 18 different compositions in a single experiment. Conducting electrochemical impedance spectroscopy to evaluate proton-electron conductivity.

Examining surface morphology and composition using scanning electron microscopy and X-ray diffraction. Performing hydrogen permeability **tests** on selected bulk compositions to meet industrial application requirements.

Master's Thesis Researcher | Mugla Sitki Kocman University | Sep 2020 – Jan 2025
Conducted a research project on the synthesis and characterization of nanocomposite tungsten oxide-silicon dioxide thin films using the sol-gel dip coating method. Investigated tungsten oxide, a versatile material with multiple crystal structures, optical and electrical properties, and chemical stability. Synthesized nanocomposite films through a one-step sol-gel process, dissolving tungsten chromate in tetraethyl orthosilicate and alcohol under base-catalyzed conditions with ammonium hydroxide. Analyzed microstructural properties using SEM observations. Measured optical properties using spectrophotometers. Evaluated photocatalytic activity by monitoring contact angles and the degradation of methylene blue under artificial daylight irradiation.

Internships

Intern | Mugla University | Jun 2019 – Sep 2019

Conducted a laboratorial experiments on "Measuring Hydrogen permeation rate and protonic conductivity measurement using ceramic membrane for Hydrogen separation" at the Metallurgical and Materials engineering department

Mechanical Engineer Designer | Rotafilo Havacilik | Jun 2018 – Sep 2018

Designed and developed metal parts manufacturing for Aircraft & Engine Tooling, Ground Support Equipment, and ATA Spec 300 Shipping Cases using Solidworks

Ensured quality control of manufactured parts

Mechanical Designer | Smart Mach | Jun 2015 – Sep 2015

Designed and developed CNC router machines for manufacturing

Technical Skills

R language. for data analysis and modeling

Solidworks. for mechanical design, assembly, and simulation analysis

PhreeqC. for solution chemistry simulation based on thermodynamics calculations

Profex. for XRD spectra analysis and interpretation

Design Expert. for designing experiments using statistical models

Certifications

Google Data Analysis Diploma (3 out of 8 courses) | Coursera | Sep 2022

Salesforce Certified Administrator (SCA) | |Salesforce | Nov 2022

Generative AI |Linkedin Learning| May 2023

Market research |Udemy | May 2023

Languages

Arabic, English and Turkish